Journal of Solid Mechanics Vol. 9, No. 4 (2017) pp. 707-729

Nonlocal Piezomagnetoelasticity Theory for Buckling Analysis of Piezoelectric/Magnetostrictive Nanobeams Including Surface Effects

A. Ghorbanpour Arani [1, 2 *], M. Abdollahian [1], A.H. Rahmati [1]

[1] *Faculty of Mechanical Engineering, University of Kashan, Kashan, Iran*
[2] *Institute of Nanoscience & Nanotechnology, University of Kashan, Kashan, Iran*

Received 4 July 2017; accepted 6 September 2017

ABSTRACT

This paper presents the surface piezomagnetoelasticity theory for size-dependent buckling analysis of an embedded piezoelectric/magnetostrictive nanobeam (PMNB). It is assumed that the subjected forces from the surrounding medium contain both normal and shear components. Therefore, the surrounded elastic foundation is modeled by Pasternak foundation. The nonlocal piezomagnetoelasticity theory is applied so as to consider the small scale effects. Based on Timoshenko beam (TB) theory and using energy method and Hamilton's principle the motion equations are obtained. By employing an analytical method, the critical magnetic, electrical and mechanical buckling loads of the nanobeam are yielded. Results are presented graphically to show the influences of small scale parameter, surrounding elastic medium, surface layers, and external electric and magnetic potentials on the buckling behaviors of PMNBs. Results delineate the significance of surface layers and external electric and magnetic potentials on the critical buckling loads of PMNBs. It is revealed that the critical magnetic, electrical and mechanical buckling loads decrease with increasing the small scale parameter. The results of this work is hoped to be of use in micro/nano electro mechanical systems (MEMS/NEMS) especially in designing and manufacturing electromagnetoelastic sensors and actuators.

Keywords : Magnetostrictive piezoelectric; Nanobeam; Surface effect; Nonlocal piezomagnetoelasticity theory; Buckling.

1 INTRODUCTION

OVER the last decade, novel accomplishments in nanomanufacturing and nanostructures fabrication have revolutionized various fields of engineering including mechanics, bio-engineering and electronics, and made it possible to utilize micro- and nano-structured materials in the frame of micro- and nano-devices. As a result, there has been an increasing demand to predict behavior of these materials in practical circumstances. Motivated by this aim, diverse models and theories has established to demonstrate their mechanical and electrical characteristics of micro- and nano-structured materials. Compare to large scale beams, atomic scale of the nanobeams has made a difference in the reaction of these structures to applied forces. Therefore, Eringen [1] presented a nonlocal elasticity

*Corresponding author. Tel.: +98 31 55912450; Fax: +98 31 55912424.
E-mail address: aghorban@kashanu.ac.ir (A.Ghorbanpour Arani).

theory in which the stress at any point of the beam is a function of strains at all points of the beam. This notion is in sharp contrast with classical continuum theories that state the stress at a point is just contingent on the strain at that point. Aydogdu [2] implemented a generalized nonlocal beam theory to investigate bending, buckling and free vibration of nanobeams. A nonlocal shear deformation beam theory was used by Thai [3] to present analytical solutions of deflection, buckling load, and natural frequency for a simply supported beam. Nazemezhad and Hosseini-Hashemi [4] studied the small scale effects on the nonlinear free vibration of nanoscale functionally graded (FG) Euler–Bernoulli beams (EBB) with von karman type nonlinearity. Rahmani and Pedram [5] applied nonlocal elasticity and TB model to investigate the effects of length scale parameter and length-to-thickness ratio on the vibration characteristics of functionally graded material (FGM) nanobeams with simply supported boundary conditions. A gradient model for Timoshenko nanobeams based on a consistent thermodynamic approach was developed by Sciarra and Barretta [6] to investigate static bending of the nanobeam. They introduced two nonlocal parameters in their model so as to separate the nonlocal contributions due to the normal and transverse shear strains and concluded that the classical TB models overestimate the static responses with respect to the proposed model. Akgoz and Civalek [7] developed a size-dependent higher-order shear deformation beam model based on modified strain gradient theory to investigate the static bending and free vibration behavior of simply supported microbeams. This model captured both the microstructural and shear deformation effects without the need for any shear correction factors. Buckling analysis of microbeams was presented by Mohammad-Abadi and Daneshmehr [8] based on modified couple stress theory. They demonstrated that considering size effect increases the stiffness of microbeams. Interesting type of functionally materials, piezoelectric materials are used in MEMS/NEMS technology. Their capacity as sensors and actuators has yielded by providing a transformation between electrical and mechanical energy [9]. Nano-piezoelectric structures respond better to small forces, display improved piezoelectric properties and can be used for powering wireless sensors, microrobots, MEMS/MEMS, and bioimplantable devices [10-12] due to their small size. Therefore, there has been a great tendency among researchers to consider the effects of piezoelectric characteristics on nanostructured materials formulations. In this regard, Ghorbanpour Arani et al. [13] implemented nonlocal elasticity and piezoelasticity theories to investigate electro-thermo-torsional buckling response of a double-walled boron nitride nanotube. They used the first order shear deformation theory to take into account the relationship between the piezoelectric coefficient of armchair boron nitride nanotubes and stresses. A study on the buckling and dynamic stability of a piezoelectric viscoelastic nanobeam subjected to van der Waals forces was presented by Chen et al. [14]. In their probe Galerkin method and EBB hypothesis were used to investigate the buckling, post-buckling and nonlinear dynamic stability of the nanobeam. Asemi et al. [15] presented a nonlinear continuum model for the large amplitude vibration of nanoelectromechanical resonators using piezoelectric nanofilms under external electric voltage. They showed that the small scale effects are more pronounced when the piezoelectric nanoresonator is subjected to higher electrical loads.

In order to present a more accurate model, it is really crucial to consider the effects of the applied forces from the medium in which nanostructure is embedded. Winkler model has been utilized in many cases to simulate the surrounding impacts as a normal pressure. A research on the buckling of single walled carbon nanotube embedded in Winkler foundation was carried out by Pradhan and Reddy [16] using differential transformation method. They indicated that critical buckling load increases with an increase in Winkler modulus for various boundary conditions. Han and Lu [17] used a Winkler model to study the torsional buckling of a double-walled carbon nanotube. Apart from normal pressure, the subjected force from the surrounding may contain a shear component. In such case Winkler model is not precise to resemble the medium effect. A Pasternak model has been presented to satisfy accuracy of simulation. A number of researches are found in the literature in which Pasternak model has been applied to mimic different nanostructures behaviors. Rahmati and Mohammadimehr [18] presented a Pasternak model for a non-uniform and non-homogeneous nanorod under electro-thermo-mechanical loadings. They concluded that any increase in either Winkler or Pasternak coefficient is accompanied by a growth in natural frequency. Abdollahian et al. [19] considered the effect of Pasternak foundation on the wave propagation of three-walled boron nitride nanotubes conveying viscous fluid based on nonlocal elasticity cylindrical shell theory. The thermal buckling of nanoplates lying on Winkler–Pasternak elastic substrate medium was investigated by Zenkour and Sobhy [20], using the sinusoidal shear deformation plate theory. In comparison with conventional scale materials, the surface to volume ratio of nanostructured materials is obviously considerable, hence, it would not be sensible to neglect the influence of surface energy in formulation of the nanostructures as it assumes in classical continuum theories [21-25]. Consequently, researchers have presented novel models for various nanostructures through which the surface effect is taken into account. Herein, Moshtaghin et al. [21] used modified Hill's condition with size-dependent moduli to study the effects of surface residual stress as well as surface elasticity on the overall yield strength of nanoporous metal matrices containing aligned cylindrical nanovoids. Based on surface piezoelasticity model, the anti-plane or horizontally polarized shear waves propagation in an infinite piezoelectric

plate of nano-thickness were investigated by Zhang et al. [22] to show the surface effect on wave characteristics. The cooperative effects of surface piezoelectricity and nonlocal small-scale on the propagation characteristics of elastic waves in an infinite piezoelectric nanoplate were investigated by Zhang et al.[23]. They concluded that both the nonlocal scale parameter and surface piezoelectricity have significant influence on the size-dependent properties of dispersion behaviors. Hosseini-Hashemi et al. [24] presented a comprehensive analytical model to study the surface effects, including surface elasticity, surface tension and surface density, on the nonlinear free vibration of FG nanoscale EBBs using nonlocal elasticity. They considered the von Karman geometric nonlinearity with the assumption of cubic variation of normal stress through the thickness. Ansari and Sahmani [25] employed a continuum elasticity model on the basis of Gurtin–Murdoch elasticity theory to analyze influences of surface stress on the bending and buckling responses of nanobeams. Magnetostrictive materials are new smart materials which are capable of magneto-mechanical coupling [26]. This magnetization and strain coupling as well as the ability of miniaturization and arbitrary shaping have provided these materials with phenomenal characteristics to be utilized in various NEMS and MEMS-based devices as stress and torque sensors and energy harvesters [26-28]. The magneto-electro-elastic (MEE) or piezoelectric/magnetostrictive materials are novel materials which benefit from advantages of both piezoelectric and magnetostrictive materials. These materials are well known for their exceptional ability to convert energy among electrical, magnetic and elastic forms, generated from possession of piezoelectric, piezomagnetic, magnetoelectric and magnetoelectroelastic couplings. This ability of MEE materials has caused them to be regarded as an appropriate class of materials for a wide range of application including sensors, actuators, electronic memory devices and electronic instrumentations [29-31]. These applications have been accompanied among researchers to investigate mechanical behavior of MEE materials; vibration, buckling and wave propagation [32-35]. Though, a limited number of studies have carried out on MEE nanostructures. Li et al. [36] implemented nonlocal Mindlin theory to analyze buckling and free vibration of MEE nanoplate resting on Pasternak foundation. They showed that the buckling load and vibration frequency of MEE nanoplate decrease linearly with electric potential and increase with magnetic potential. Also, the importance of the electric and magnetic loadings in free vibration of MEE nanobeams illustrated by Ke and Wang [37] using the nonlocal and TB theories.

However, to date, no reference has been made so far in the literature on the buckling analysis of PMNBs including surface effects. Since PMNBs can be used in many engineering and medical applications especially in NEMS, in order to improve the optimum design of such devices the problem of buckling analysis of PMNBs becomes significant. Motivated by these considerations, in this research, nonlocal piezomagnetoelasticity theory is applied to study the small scale effects on the buckling characteristics of PMNBs embedded on a Pasternak elastic medium. Based on surface piezomagnetoelasticity theory the effects of surface layers are taken into account. Using Hamilton's principle, the motion equations are derived and then, an analytical method is presented to estimate the critical magnetic, electrical and mechanical buckling loads.

2 SUBMISSIONS OF PAPERS

The coordinate system of the central axis of nanobeam is x , y and z that are taken for the length, width and thickness of the nanobeam, respectively (See Fig. 1). Consider a PMNB as depicted in Fig. 1 which shows the geometrical parameters of length L and rectangular cross section of thickness h and width b. The PMNB is rested on an elastic medium which is simulated by Pasternak foundation and it is also subjected to external electric and magnetic potentials. As is well known, this foundation model is both capable of transverse shear and normal loads.

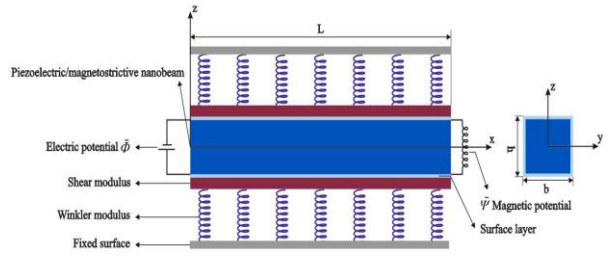

Fig.1
Schematic view of embedded PMNB with surface layers.

According to TB theory which is used in the present formulation, the displacement of any arbitrary point of the PMNB along x , y and z directions (u_x ,u_y and u_z) can be expressed as [38]:

$$u_x\left(x,z,t\right)=u\left(x,t\right)+z\,\varphi\left(x,t\right), \tag{1a}$$

$$u_y\left(x,z,t\right)=0, \tag{1b}$$

$$u_z\left(x,z,t\right)=w\left(x,t\right), \tag{1c}$$

where $u\left(x,t\right)$ and $w\left(x,t\right)$ are the displacement components of the mid-plane in the x and z directions, respectively. Also, $\varphi\left(x,t\right)$ is the rotation angle of the cross section. Considering Eq. (1) the nonzero nonlinear strain–displacement relationship of von Karman type is given by:

$$\varepsilon_{xx}=\frac{\partial u}{\partial x}+z\,\frac{\partial \varphi}{\partial x}+\frac{1}{2}\left(\frac{\partial w}{\partial x}\right)^2, \tag{2a}$$

$$\gamma_{xz}=2\varepsilon_{xz}=\frac{\partial w}{\partial x}+\varphi. \tag{2b}$$

Moreover, the electric potential $\tilde{\Phi}\left(x,z,t\right)$ and magnetic potential $\tilde{\Psi}\left(x,z,t\right)$ are assumed as [37]:

$$\tilde{\Phi}\left(x,z,t\right)=-\cos\left(\beta z\right)\phi\left(x,t\right)+\frac{2z\,\phi_0}{h}, \tag{3a}$$

$$\tilde{\Psi}\left(x,z,t\right)=-\cos\left(\beta z\right)\psi\left(x,t\right)+\frac{2z\,\psi_0}{h}, \tag{3b}$$

where $\beta=\pi/h$, $\phi\left(x,t\right)$ and $\psi\left(x,t\right)$ are the spatial variation of the electric and magnetic potential in x-direction, respectively [36, 37]. Also, ϕ_0 and ψ_0 denote the initial applied electric and magnetic potentials, respectively.

The electric field (E_i) and magnetic field (H_i) components can be obtained from the following relations as [37]:

$$E_i=-\tilde{\Phi}_{,i}, \tag{4a}$$

$$H_i=-\tilde{\Psi}_{,i}. \tag{4b}$$

Using Eqs. (4), the following relations may be obtained as:

$$E_x=-\frac{\partial\tilde{\Phi}}{\partial x}=\cos\left(\beta z\right)\frac{\partial\phi}{\partial x}, \tag{5a}$$

$$E_z=-\frac{\partial\tilde{\Phi}}{\partial z}=-\beta\sin\left(\beta z\right)\phi+\frac{2\phi_0}{h}, \tag{5b}$$

$$H_x=-\frac{\partial\tilde{\Psi}}{\partial x}=\cos\left(\beta z\right)\frac{\partial\psi}{\partial x}, \tag{5c}$$

$$H_z=-\frac{\partial\tilde{\Psi}}{\partial z}=-\beta\sin\left(\beta z\right)\psi+\frac{2\psi_0}{h}. \tag{5d}$$

3 NONLOCAL PIEZOMAGNETOELASTICITY THEORY

The small length scale involved in nanotechnology has questioned the applicability of the classical mechanics model. The small size of the nano-structure materials is very important in nanotechnology problems. As this scale is ignored in the classical mechanics model, the nonlocal piezomagnetoelasticity theory is employed for PMNBs. For a homogeneous and nonlocal piezoelectric/magnetostrictive solid without body force, the following equations can be written [13, 37, 39]:

$$\sigma_{ij} = \int_V \alpha\left(\left|x'-x\right|.\tau\right)\left[c_{ijkl}\varepsilon_{kl} - e_{kij}E_k\left(x'\right) - f_{kij}H_k\left(x'\right)\right]dx', \tag{6a}$$

$$D_i = \int_V \alpha\left(\left|x'-x\right|.\tau\right)\left[e_{kij}\varepsilon_{kl} + h_{ik}E_k\left(x'\right) + g_{ik}H_k\left(x'\right)\right]dx', \tag{6b}$$

$$B_i = \int_V \alpha\left(\left|x'-x\right|.\tau\right)\left[f_{kij}\varepsilon_{kl} + g_{ik}E_k\left(x'\right) + \mu_{ik}H_k\left(x'\right)\right]dx', \tag{6c}$$

$$\sigma_{ij,j} = \rho\ddot{u}_i, D_{i,i} = 0, H_{i,i} = 0, \tag{6d}$$

where $\sigma_{ij}, \varepsilon_{ij}, D_i$ and H_i are the stress, strain, electric displacement and magnetic induction components, respectively; Also, $c_{ijkl}, e_{kij}, h_{ik}, f_{kij}, g_{ik}$ and μ_{ik} are elastic, piezoelectric, dielectric, piezomagnetic, magnetoelectric and magnetic constants, respectively [34-37]; $\alpha\left(\left|x'-x\right|,\tau\right)$ is the nonlocal attenuation function; $\left|x'-x\right|$ is the Euclidean distance; $\tau = e_0 a/l$ is the scale coefficient, where l is the external characteristics of length. It is Also worth mentioning that, $e_0 a$ is the nonlocal parameter, e_0 is a material constant determined experimentally or approximated by matching the dispersion curves of the (plane/beam) waves with those of the atomic lattice dynamics and a is the internal characteristic length .The nonlocal parameter is obtained using molecular dynamics, experimental results, experimental studies and molecular structure mechanics [34, 37].

The According to linear elasticity, the nonzero components of stresses, electric displacements and magnetic inductions for the bulk material can be written as follows [37]:

$$\sigma_{xx}^b - \left(e_0 a\right)^2 \nabla^2 \sigma_{xx}^b = c_{11}\varepsilon_{xx} - e_{31}E_z - f_{31}H_z, \tag{7a}$$

$$\sigma_{xz}^b - \left(e_0 a\right)^2 \nabla^2 \sigma_{xz}^b = c_{44}\gamma_{xz} - e_{15}E_x - f_{15}H_x, \tag{7b}$$

$$D_x^b - \left(e_0 a\right)^2 \nabla^2 D_x^b = e_{15}\gamma_{xz} + h_{11}E_x + g_{11}H_x, \tag{7c}$$

$$D_z^b - \left(e_0 a\right)^2 \nabla^2 D_z^b = e_{31}\varepsilon_{xx} + h_{33}E_z + g_{33}H_z, \tag{7d}$$

$$B_x^b - \left(e_0 a\right)^2 \nabla^2 B_x^b = f_{15}\gamma_{xz} + g_{11}E_x + \mu_{11}H_x, \tag{7e}$$

$$B_z^b - \left(e_0 a\right)^2 \nabla^2 B_z^b = f_{31}\varepsilon_{xx} + g_{33}E_z + \mu_{33}H_z. \tag{7f}$$

4 SURFACE LAYERS

Based on nonlocal piezomagnetoelasticity theory the constitutive relations for the surface layer can be written as [22, 23]:

$$\sigma_{xx}^{s}-\left(e_0a\right)^2\nabla^2\sigma_{xx}^{s}=\sigma_{xx}^{0}+c_{11}^{s}\varepsilon_{xx}+c_{13}^{s}\varepsilon_{zz}-e_{31}^{s}E_z-f_{31}^{s}H_z, \tag{8a}$$

$$\sigma_{xz}^{s}-\left(e_0a\right)^2\nabla^2\sigma_{xz}^{s}=\sigma_{xz}^{0}+c_{44}^{s}\gamma_{xz}-e_{15}^{s}E_x-f_{15}^{s}H_x, \tag{8b}$$

$$D_{x}^{s}-\left(e_0a\right)^2\nabla^2D_{x}^{s}=D_{x}^{0}+e_{15}^{s}\gamma_{xz}+h_{11}^{s}E_x+g_{11}^{s}H_x, \tag{8c}$$

$$D_{z}^{s}-\left(e_0a\right)^2\nabla^2D_{z}^{s}=D_{z}^{0}+e_{31}^{s}\varepsilon_{xx}+e_{33}^{s}\varepsilon_{zz}+h_{33}^{s}E_z+g_{33}^{s}H_z, \tag{8d}$$

$$B_{x}^{s}-\left(e_0a\right)^2\nabla^2B_{x}^{s}=B_{x}^{0}+f_{15}^{s}\gamma_{xz}+g_{11}^{s}E_x+\mu_{11}^{s}H_x, \tag{8e}$$

$$B_{z}^{s}-\left(e_0a\right)^2\nabla^2B_{z}^{s}=B_{z}^{0}+f_{31}^{s}\varepsilon_{xx}+f_{33}^{s}\varepsilon_{zz}+g_{33}^{s}E_z+\mu_{33}^{s}H_z. \tag{8f}$$

where the upper index "s" indicates the coefficients of the surface layers. Also, it is worth mentioning that in the present study $D_x^0, D_z^0, B_x^0, B_z^0, \sigma_{xz}^0$ are assumed to be zero and only the effect of σ_{xx}^0 as the surface residual stress is considered.

According to Gurtin-Murdoch model and unlike classical plate theories [35, 40, 41], σ_{zz} is not equal to zero. Indeed, the stress component σ_{zz} varies linearly along the graphene sheet thickness and satisfies the balance condition on the surfaces which can be expressed as the following relation [40]:

$$\sigma_{zz}=\frac{1}{2}\left[\left(\frac{\partial\sigma_{xz}^{s+}}{\partial x}\right)+\left(\frac{\partial\sigma_{xz}^{s-}}{\partial x}\right)\right]+\frac{z}{h}\left[\left(\frac{\partial\sigma_{xz}^{s+}}{\partial x}\right)-\left(\frac{\partial\sigma_{xz}^{s-}}{\partial x}\right)\right]. \tag{9}$$

Using Eq. (8), Eq. (9) can be rewritten as:

$$\sigma_{zz}=\frac{2z}{h}\left(c_{44}^{s}\left(\frac{\partial^2 w}{\partial x^2}+\frac{\partial\varphi}{\partial x}\right)-e_{15}^{s}\cos\left(\beta z\right)\frac{\partial^2\phi}{\partial x^2}-f_{15}^{s}\cos\left(\beta z\right)\frac{\partial^2\psi}{\partial x^2}\right). \tag{10}$$

By introducing σ_{zz} the stress, electric displacement and magnetic induction components, introduced in Eqs. (7) and (8) for both bulk material and surface layers, can be rewritten as presented in Appendix A.

5 EQUATIONS OF MOTION

The strain energy of the PMNB can be written as follows:

$$\begin{aligned}\Pi_s=&\frac{1}{2}\int_0^L\int_A\left(\sigma_{ij}\varepsilon_{ij}-D_iE_i-B_iH_i\right)dA\,dx\\&+\frac{1}{2}\left(\int_0^L\int_{S^+}\left(\sigma_{ij}^{S^+}\varepsilon_{ij}-D_i^{S^+}E_i-B_i^{S^+}H_i\right)dS^+dx+\int_0^L\int_{S^-}\left(\sigma_{ij}^{S^-}\varepsilon_{ij}-D_i^{S^-}E_i-B_i^{S^-}H_i\right)dS^-dx\right).\end{aligned} \tag{11}$$

The external work due to the Pasternak surrounding elastic medium is written as:

$$W_{ext}=\int_0^L\left[\left(-k_w w+k_g\frac{\partial^2 w}{\partial x^2}\right)w\right]dx. \tag{12}$$

where k_w is the spring constant of Winkler type, k_g denotes the shear constant of Pasternak type and f is the x-component of the body force per unit length along the x- axis.

Substituting Eqs. (11) and (12) into the Hamilton's principle ($\delta\int_0^T \left(-\Pi_s + W_{ext}\right)dt = 0$), integrating by part and setting the coefficients of $\delta u, \delta w, \delta\varphi, \delta\phi$ and $\delta\psi$ to zero, the governing equations of motion can be obtained as follows:

$$\delta u : \frac{\partial N_x}{\partial x} + f = 0, \tag{13a}$$

$$\delta w : \frac{\partial}{\partial x}\left(N_x \frac{\partial w}{\partial x}\right) + \frac{\partial Q_x}{\partial x} - k_w w + k_g \frac{\partial^2 w}{\partial x^2} = 0, \tag{13b}$$

$$\delta\varphi : \frac{\partial M_x}{\partial x} - Q_x = 0, \tag{13c}$$

$$\delta\phi : \int_A \left[-\frac{\partial D_x^b}{\partial x}\cos(\beta z) - D_z^b \beta \sin(\beta z)\right]dA + \int_S \left[-\frac{\partial D_x^s}{\partial x}\cos(\beta z) - D_z^s \beta \sin(\beta z)\right]dS = 0, \tag{13d}$$

$$\delta\psi : \int_A \left[-\frac{\partial B_x^b}{\partial x}\cos(\beta z) - B_z^b \beta \sin(\beta z)\right]dA + \int_S \left[-\frac{\partial B_x^s}{\partial x}\cos(\beta z) - B_z^s \beta \sin(\beta z)\right]dS = 0. \tag{13e}$$

Also, the associated boundary conditions may be obtained as follows:

$$x = 0, L: \quad \delta u = 0 \quad OR \quad N_x = 0, \tag{14a}$$

$$x = 0, L: \quad \delta w = 0 \quad OR \quad N_x \frac{\partial w}{\partial x} + Q_x = 0, \tag{14b}$$

$$x = 0, L: \quad \delta\varphi = 0 \quad OR \quad M_x = 0, \tag{14c}$$

$$x = 0, L: \quad \delta\phi = 0 \quad OR \quad \int_0^L \left(D_x^b + D_x^s\right)\cos(\beta z)dz = 0, \tag{14d}$$

$$x = 0, L: \quad \delta\psi = 0 \quad OR \quad \int_0^L \left(B_x^b + B_x^s\right)\cos(\beta z)dz = 0, \tag{14e}$$

In which:

$$\begin{aligned}&\left(1-(e_0 a)^2\nabla^2\right)N_x = \left(1-(e_0 a)^2\nabla^2\right)\left(\int_A \sigma_{xx}dA + \int_s \sigma_{xx}^s dS\right) = \\ &\left(bA_{11} + 2\tilde{c}_{11}^s(b+h)\right)\left(\frac{\partial u}{\partial x} + \frac{1}{2}\left(\frac{\partial w}{\partial x}\right)^2\right) + 2(b+h)\sigma_{xx}^0 + 4(b+h)\left(\frac{\tilde{e}_{31}^s\phi_0}{h} - \frac{\tilde{f}_{31}^s\psi_0}{h}\right) \\ &+2b\left(\tilde{e}_{31}\phi_0 + \tilde{f}_{31}\psi_0\right),\end{aligned} \tag{15a}$$

$$\left(1-\left(e_0a\right)^2\nabla^2\right)M_x=\left(1-\left(e_0a\right)^2\nabla^2\right)\left(\int_A\sigma_{xx}zdA+\int_s\sigma_{xx}^szdS\right)=$$
$$\left(bD_{11}+\frac{bh^2}{2}\tilde{c}_{11}^s+\tilde{c}_{11}^s\frac{h^3}{6}\right)\frac{\partial\varphi}{\partial x}+\left(b\tilde{E}_{31}+bh\tilde{e}_{31}^s\beta+2\tilde{E}_{31}^s\right)\phi+\left(b\tilde{F}_{31}+bh\tilde{f}_{31}^s\beta+2\tilde{F}_{31}^s\right)\psi$$
$$+\left(\frac{bh^2}{6}\frac{c_{13}}{c_{33}}+bh\frac{c_{13}^s}{c_{33}}+\frac{c_{13}^s}{c_{33}}\frac{h^2}{3}\right)c_{44}^s\left(\frac{\partial^2w}{\partial x^2}+\frac{\partial\varphi}{\partial x}\right)-\left(\frac{2b}{h}\frac{c_{13}}{c_{33}}E_{25}^s+\frac{c_{13}^s}{c_{33}}\frac{4}{h}E_{25}^s\right)\frac{\partial^2\phi}{\partial x^2}$$
$$-\left(\frac{2b}{h}\frac{c_{13}}{c_{33}}F_{25}^s+\frac{c_{13}^s}{c_{33}}\frac{4}{h}F_{25}^s\right)\frac{\partial^2\psi}{\partial x^2}\tag{15b}$$

$$\left(1-\left(e_0a\right)^2\nabla^2\right)Q_x=\left(1-\left(e_0a\right)^2\nabla^2\right)\left(k_s\int_A\sigma_{xz}dA+\int_s\sigma_{xz}^sdS\right)=2\sigma_{xz}^0\left(b+h\right)+$$
$$\left(bk_sA_{44}+2c_{44}^s\left(b+h\right)\right)\left(\frac{\partial w}{\partial x}+\varphi\right)-\left(bk_sE_{15}+2E_{15}^s\right)\frac{\partial\phi}{\partial x}-\left(bk_sF_{15}+2F_{15}^s\right)\frac{\partial\psi}{\partial x},\tag{15c}$$

$$\left(1-\left(e_0a\right)^2\nabla^2\right)\left(\int_AD_x^b\cos\left(\beta z\right)dA+\int_sD_x^s\cos\left(\beta z\right)dS\right)=\left(bE_{15}+2E_{15}^s\right)\left(\frac{\partial w}{\partial x}+\varphi\right)$$
$$+\left(bX_{11}+2X_{11}^s\right)\frac{\partial\phi}{\partial x}+\left(bY_{11}+2Y_{11}^s\right)\frac{\partial\psi}{\partial x},\tag{15d}$$

$$\left(1-\left(e_0a\right)^2\nabla^2\right)\left(\int_AD_x^b\beta\sin\left(\beta z\right)dA+\int_sD_x^s\beta\sin\left(\beta z\right)dS\right)=\left(b\tilde{E}_{31}+2\tilde{E}_{31}^{ts}+bh\beta\tilde{e}_{31}^{ts}\right)\frac{\partial\varphi}{\partial x}$$
$$-\left(b\tilde{X}_{33}+2\tilde{X}_{33}^s+2b\beta^2\tilde{h}_{33}^s\right)\phi-\left(b\tilde{Y}_{33}+2\tilde{Y}_{33}^s+2b\beta^2\tilde{g}_{33}^s\right)\psi$$
$$+\left(\frac{2b}{h}\frac{E_{33}}{c_{33}}+\frac{4}{h}\frac{E_{33}^s}{c_{33}}+2b\beta\frac{e_{33}^s}{c_{33}}\right)c_{44}^s\left(\frac{\partial^2w}{\partial x^2}+\frac{\partial\varphi}{\partial x}\right)-\left(\frac{e_{33}}{c_{33}}\frac{2b}{h}Z_1+\frac{e_{33}^s}{c_{33}}\frac{4}{h}Z_1\right)\frac{\partial^2\phi}{\partial x^2}\tag{15e}$$
$$-\left(\frac{e_{33}}{c_{33}}\frac{2b}{h}Z_2+\frac{e_{33}^s}{c_{33}}\frac{4}{h}Z_2\right)\frac{\partial^2\psi}{\partial x^2}$$

$$\left(1-\left(e_0a\right)^2\nabla^2\right)\left(\int_AB_x^b\cos\left(\beta z\right)dA+\int_sB_x^s\cos\left(\beta z\right)dS\right)=\left(bF_{15}+2F_{15}^s\right)\left(\frac{\partial w}{\partial x}+\varphi\right)$$
$$+\left(bY_{11}+2Y_{11}^s\right)\frac{\partial\phi}{\partial x}+\left(bT_{11}+2T_{11}^s\right)\frac{\partial\psi}{\partial x},\tag{15f}$$

$$\left(1-\left(e_0a\right)^2\nabla^2\right)\left(\int_AB_x^b\beta\sin\left(\beta z\right)dA+\int_sB_x^s\beta\sin\left(\beta z\right)dS\right)=\left(b\tilde{F}_{31}+2\tilde{F}_{31}^{ts}+bh\beta\tilde{f}_{31}^{ts}\right)\frac{\partial\varphi}{\partial x}$$
$$-\left(b\tilde{Y}_{33}+2\tilde{Y}_{33}^{ts}+2b\beta^2\tilde{g}_{33}^{ts}\right)\phi-\left(b\tilde{T}_{33}+2\tilde{T}_{33}^s+2b\beta^2\tilde{\mu}_{33}^s\right)\psi$$
$$+\left(\frac{2b}{h}\frac{F_{33}}{c_{33}}+\frac{4}{h}\frac{F_{33}^s}{c_{33}}+2b\beta\frac{f_{33}^s}{c_{33}}\right)c_{44}^s\left(\frac{\partial^2w}{\partial x^2}+\frac{\partial\varphi}{\partial x}\right)-\left(\frac{f_{33}}{c_{33}}\frac{2b}{h}Z_1+\frac{f_{33}^s}{c_{33}}\frac{4}{h}Z_1\right)\frac{\partial^2\phi}{\partial x^2}\tag{15g}$$
$$-\left(\frac{f_{33}}{c_{33}}\frac{2b}{h}Z_2+\frac{f_{33}^s}{c_{33}}\frac{4}{h}Z_2\right)\frac{\partial^2\psi}{\partial x^2}$$

where k_s is the shear correction factor and:

$$
\begin{aligned}
&\left(A_{11},D_{11}\right)=\int_{-h/2}^{h/2}\tilde{c}_{11}\left(1,z^{2}\right)dz\,,A_{44}=\int_{-h/2}^{h/2}c_{44}dz\,,\\
&\left(\tilde{E}_{31},\tilde{E}_{31}^{s},\tilde{E}_{31}^{\prime s},E_{33},E_{33}^{s},\tilde{F}_{31},\tilde{F}_{31}^{s},\tilde{F}_{31}^{\prime s},F_{33},F_{33}^{s}\right)=\int_{-h/2}^{h/2}\left(\tilde{e}_{31},\tilde{e}_{31}^{s},\tilde{e}_{31}^{\prime s},e_{33},e_{33}^{s},\tilde{f}_{31},\tilde{f}_{31}^{s},\tilde{f}_{31}^{\prime s},f_{33},f_{33}^{s}\right)\beta\sin\left(\beta z\right)zdz\,,\\
&\left(E_{15}^{s},E_{25}^{s}\right)=\int_{-h/2}^{h/2}e_{15}^{s}\cos\left(\beta z\right)\left(1,z^{2}\right)dz\,,\left(F_{15}^{s},F_{25}^{s}\right)=\int_{-h/2}^{h/2}f_{15}^{s}\cos\left(\beta z\right)\left(1,z^{2}\right)dz\,,\\
&\left(E_{15},F_{15}\right)=\int_{-h/2}^{h/2}\left(e_{15},f_{15}\right)\cos\left(\beta z\right)dz\,,\\
&\left(X_{11},Y_{11},T_{11},X_{11}^{s},Y_{11}^{s},T_{11}^{s}\right)=\int_{-h/2}^{h/2}\left(h_{11},g_{11},\mu_{11},h_{11}^{s},g_{11}^{s},\mu_{11}^{s}\right)\left[\cos\left(\beta z\right)\right]^{2}dz\,,\\
&\left(\tilde{X}_{33},\tilde{X}_{33}^{s},\tilde{Y}_{33},\tilde{Y}_{33}^{s},\tilde{Y}_{33}^{\prime s},\tilde{T}_{33},\tilde{T}_{33}^{s}\right)=\int_{-h/2}^{h/2}\left(\tilde{h}_{33},\tilde{h}_{33}^{s},\tilde{g}_{33},\tilde{g}_{33}^{s},\tilde{g}_{33}^{\prime s},\tilde{\mu}_{33},\tilde{\mu}_{33}^{s}\right)\left[\beta\sin\left(\beta z\right)\right]^{2}dz\,,\\
&\left(Z_{1},Z_{2}\right)=\int_{-h/2}^{h/2}\left(e_{15}^{s},f_{15}^{s}\right)\beta\sin\left(\beta z\right)\cos\left(\beta z\right)zdz\,,
\end{aligned}
\tag{16}
$$

The other parameters used in Eqs. (15) and (16) are defined in Eq. (A.13) of Appendix A. It is also worth mentioning that Eqs. (15) are rewritten in Appendix B.

The following dimensionless parameters are defined as:

$$
\begin{aligned}
&X=\frac{x}{L},W=\frac{w}{h},\mu=\frac{e_{0}a}{L},\eta=\frac{L}{h},\Phi=\varphi,\Theta=\frac{\phi}{\phi_{m}},\Psi=\frac{\psi}{\psi_{m}},\phi_{m}=\sqrt{\frac{A_{11}}{\tilde{X}_{33}}},\\
&\psi_{m}=\sqrt{\frac{A_{11}}{\tilde{T}_{33}}},\left(\bar{A}_{44},\bar{D}_{11}\right)=\left(\frac{A_{44}}{A_{11}},\frac{D_{11}}{A_{11}h^{2}}\right),\left(\bar{E}_{25}^{s},\bar{F}_{25}^{s}\right)=\left(\frac{E_{25}^{s}\phi_{m}}{A_{11}h^{3}L},\frac{F_{25}^{s}\psi_{m}}{A_{11}h^{3}L}\right),\\
&\left(\bar{E}_{15},\bar{E}_{15}^{s},\bar{\tilde{E}}_{31},\bar{\tilde{E}}_{31}^{s},\bar{E}_{33},\bar{E}_{33}^{s},\bar{\tilde{E}}_{31}^{\prime s}\right)=\left(\frac{E_{15}\phi_{m}}{A_{11}h},\frac{E_{15}^{s}\phi_{m}}{bhA_{11}},\frac{\tilde{E}_{31}\phi_{m}}{A_{11}h},\frac{\tilde{E}_{31}^{s}\phi_{m}}{A_{11}bh},\frac{E_{33}\phi_{m}}{A_{11}h},\frac{E_{33}^{s}\phi_{m}}{A_{11}bh},\frac{\tilde{E}_{31}^{\prime s}\phi_{m}}{A_{11}bh}\right),\\
&\left(\bar{X}_{11},\bar{X}_{11}^{s},\bar{Y}_{11},\bar{Y}_{11}^{s}\right)=\left(\frac{X_{11}\phi_{m}^{2}}{A_{11}h^{2}},\frac{X_{11}^{s}\phi_{m}^{2}}{A_{11}bh^{2}},\frac{Y_{11}\psi_{m}\phi_{m}}{A_{11}h^{2}},\frac{Y_{11}^{s}\psi_{m}\phi_{m}}{A_{11}bh^{2}}\right),\\
&\left(\bar{\tilde{X}}_{33},\bar{\tilde{X}}_{33}^{s},\bar{\tilde{Y}}_{33},\bar{\tilde{Y}}_{33}^{s}\right)=\left(\frac{\tilde{X}_{33}\phi_{m}^{2}}{A_{11}},\frac{\tilde{X}_{33}^{s}\phi_{m}^{2}}{A_{11}b},\frac{\tilde{Y}_{33}\psi_{m}\phi_{m}}{A_{11}},\frac{\tilde{Y}_{33}^{s}\psi_{m}\phi_{m}}{A_{11}b}\right),\\
&\left(\bar{T}_{11},\bar{T}_{11}^{s},\bar{\tilde{T}}_{33},\bar{\tilde{T}}_{33}^{s}\right)=\left(\frac{T_{11}\psi_{m}^{2}}{A_{11}h^{2}},\frac{T_{11}^{s}\psi_{m}^{2}}{A_{11}bh^{2}},\frac{\tilde{T}_{33}\psi_{m}^{2}}{A_{11}},\frac{\tilde{T}_{33}^{s}\psi_{m}^{2}}{A_{11}b}\right),\\
&\bar{N}_{L}=\frac{N_{L}}{A_{11}b},K_{w}=\frac{k_{w}L^{2}}{A_{11}b},K_{g}=\frac{k_{g}}{A_{11}b},\bar{c}_{44}^{s}=\frac{\left(b+h\right)c_{44}^{s}}{bA_{11}},\\
&\left(\bar{F}_{15},\bar{F}_{15}^{s},\bar{\tilde{F}}_{31},\bar{\tilde{F}}_{31}^{s},\bar{F}_{33},\bar{F}_{33}^{s},\bar{\tilde{F}}_{31}^{\prime s}\right)=\left(\frac{F_{15}\psi_{m}}{A_{11}h},\frac{F_{15}^{s}\psi_{m}}{bhA_{11}},\frac{\tilde{F}_{31}\psi_{m}}{A_{11}h},\frac{\tilde{F}_{31}^{s}\psi_{m}}{bhA_{11}},\frac{F_{33}\psi_{m}}{A_{11}h},\frac{F_{33}^{s}\psi_{m}}{bhA_{11}},\frac{\tilde{F}_{31}^{\prime s}\psi_{m}}{bhA_{11}}\right),\\
&\left(\bar{e}_{33}^{s},\bar{f}_{33}^{s},\bar{\tilde{e}}_{31}^{s},\bar{\tilde{f}}_{31}^{s},\bar{\tilde{e}}_{31}^{\prime s},\bar{\tilde{f}}_{31}^{\prime s}\right)=\left(\frac{e_{33}^{s}\phi_{m}\beta}{A_{11}},\frac{f_{33}^{s}\psi_{m}\beta}{A_{11}},\frac{\tilde{e}_{31}^{s}\phi_{m}\beta}{A_{11}},\frac{\tilde{f}_{31}^{s}\psi_{m}\beta}{A_{11}},\frac{\tilde{e}_{31}^{\prime s}\phi_{m}\beta}{A_{11}},\frac{\tilde{f}_{31}^{\prime s}\psi_{m}\beta}{A_{11}}\right),\\
&\left(\bar{\tilde{h}}_{33}^{s},\bar{\tilde{g}}_{33}^{s},\bar{\tilde{\mu}}_{33}^{s}\right)=\left(\frac{\tilde{h}_{33}^{s}\phi_{m}^{2}\beta^{2}}{A_{11}},\frac{\tilde{g}_{33}^{s}\beta^{2}\psi_{m}\phi_{m}}{A_{11}},\frac{\tilde{\mu}_{33}^{s}\psi_{m}^{2}\beta^{2}}{A_{11}}\right)
\end{aligned}
\tag{17}
$$

In which:

$$
N_{L}=-P+2\left(b+h\right)\sigma_{xx}^{0}+4\left(b+h\right)\left(\frac{\tilde{e}_{31}^{s}\phi_{0}}{h}+\frac{\tilde{f}_{31}^{s}\psi_{0}}{h}\right)+2b\left(\tilde{e}_{31}\phi_{0}+\tilde{f}_{31}\psi_{0}\right)
\tag{18}
$$

where P is the external mechanical load subjected to the PMNB.

Substituting Eqs. (B.2)-(B.7) into Eqs. (13b)-(13e) and using Eqs. (17) yields the dimensionless motion equations as:

$$\bar{Q}_1\left(\frac{\partial^2 W}{\partial X^2}+\eta\frac{\partial \Phi}{\partial X}\right)-\bar{Q}_2\frac{\partial^2 \Theta}{\partial X^2}-\bar{Q}_3\frac{\partial^2 \Psi}{\partial X^2}+\left(1-\mu^2\frac{\partial^2}{\partial X^2}\right)\left(\bar{N}_L\frac{\partial^2 W}{\partial X^2}-K_w W+K_g\frac{\partial^2 W}{\partial X^2}\right)=0, \tag{19a}$$

$$\begin{aligned}&\bar{M}_1\frac{\partial^2 \Phi}{\partial X^2}+\bar{M}_2\eta\frac{\partial \Theta}{\partial X}+\bar{M}_3\eta\frac{\partial \Psi}{\partial X}+\bar{M}_4\left(\frac{1}{\eta}\frac{\partial^3 W}{\partial X^3}+\frac{\partial^2 \Phi}{\partial X^2}\right)\\&-\bar{M}_6\frac{\partial^3 \Theta}{\partial X^3}-\bar{M}_7\frac{\partial^3 \Psi}{\partial X^3}-\bar{Q}_1\left(\eta\frac{\partial W}{\partial X}+\eta^2\Phi\right)+\bar{Q}_2\eta\frac{\partial \Theta}{\partial X}+\bar{Q}_3\eta\frac{\partial \Psi}{\partial X}=0,\end{aligned} \tag{19b}$$

$$\begin{aligned}&\bar{D}_1\left(\frac{\partial^2 W}{\partial X^2}+\eta\frac{\partial \Phi}{\partial X}\right)+\bar{D}_2\frac{\partial^2 \Theta}{\partial X^2}+\bar{D}_3\frac{\partial^2 \Psi}{\partial X^2}+\bar{D}_4\eta\frac{\partial \Phi}{\partial X}-\bar{D}_5\eta^2\Theta-\bar{D}_6\eta^2\Psi\\&+\bar{D}_7\left(\frac{\partial^2 W}{\partial X^2}+\eta\frac{\partial \Phi}{\partial X}\right)-\bar{D}_9\frac{\partial^2 \Theta}{\partial X^2}-\bar{D}_{10}\frac{\partial^2 \Psi}{\partial X^2}=0,\end{aligned} \tag{19c}$$

$$\begin{aligned}&\bar{B}_1\left(\frac{\partial^2 W}{\partial X^2}+\eta\frac{\partial \Phi}{\partial X}\right)+\bar{B}_2\frac{\partial^2 \Theta}{\partial X^2}+\bar{B}_3\frac{\partial^2 \Psi}{\partial X^2}+\bar{B}_4\eta\frac{\partial \Phi}{\partial X}-\bar{B}_5\eta^2\Theta-\bar{B}_6\eta^2\Psi\\&+\bar{B}_7\left(\frac{\partial^2 W}{\partial X^2}+\eta\frac{\partial \Phi}{\partial X}\right)-\bar{B}_9\frac{\partial^2 \Theta}{\partial X^2}-\bar{B}_{10}\frac{\partial^2 \Psi}{\partial X^2}=0.\end{aligned} \tag{19d}$$

In which:

$$\bar{Q}_1=k_s\bar{A}_{44}+2\bar{c}^s_{44},\bar{Q}_2=k_s\bar{E}_{15}+2\bar{E}^s_{15},\bar{Q}_3=k_s\bar{F}_{15}+2\bar{F}^s_{15}, \tag{20a}$$

$$\begin{aligned}&\bar{M}_1=\bar{D}_{11}+\frac{\tilde{c}^s_{11}}{2A_{11}}+\frac{c^s_{11}}{A_{11}b}\frac{h}{6},\bar{M}_2=\bar{\tilde{E}}_{31}+\bar{\tilde{e}}^s_{31}+2\bar{\tilde{E}}^s_{31},\bar{M}_3=\bar{\tilde{F}}_{31}+\bar{\tilde{f}}^s_{31}+2\bar{\tilde{F}}^s_{31},\\&\bar{M}_4=\frac{c_{13}c^s_{44}}{6A_{11}c_{33}}+\frac{c^s_{13}c^s_{44}}{3bA_{11}c_{33}}+\frac{c^s_{13}c^s_{44}}{hA_{11}c_{33}},\bar{M}_6=\frac{2\bar{E}^s_{25}}{c_{33}}\left(c_{13}+\frac{2c^s_{13}}{b}\right),\bar{M}_7=\frac{2\bar{F}^s_{25}}{c_{33}}\left(c_{13}+\frac{2c^s_{13}}{b}\right),\end{aligned} \tag{20b}$$

$$\begin{aligned}&\bar{D}_1=\bar{E}_{15}+2\bar{E}^s_{15},\bar{D}_2=\bar{X}_{11}+2\bar{X}^s_{11},\bar{D}_3=\bar{Y}_{11}+2\bar{Y}^s_{11},\bar{D}_4=\bar{\tilde{E}}_{31}+2\bar{\tilde{E}}'^s_{31}+\bar{\tilde{e}}'^s_{31},\\&\bar{D}_5=\bar{\tilde{X}}_{33}+2\bar{\tilde{X}}^s_{33}+2\bar{\tilde{h}}^s_{33},\bar{D}_6=\bar{\tilde{Y}}_{33}+2\bar{\tilde{Y}}^s_{33}+2\bar{\tilde{g}}^s_{33},\bar{D}_7=\frac{2c^s_{44}}{c_{33}h}\left(\bar{E}_{33}+2\bar{E}^s_{33}+\bar{e}^s_{33}\right),\\&\bar{D}_9=\frac{2Z_1\phi_m^2}{A_{11}h^3c_{33}}\left(e_{33}+\frac{2}{b}e^s_{33}\right),\bar{D}_{10}=\frac{2Z_2\psi_m\phi_m}{A_{11}h^3c_{33}}\left(e_{33}+\frac{2}{b}e^s_{33}\right),\end{aligned} \tag{20c}$$

$$\begin{aligned}&\bar{B}_1=\bar{F}_{15}+2\bar{F}^s_{15},\bar{B}_2=\bar{Y}_{11}+2\bar{Y}^s_{11},\bar{B}_3=\bar{T}_{11}+2\bar{T}^s_{11},\bar{B}_4=\bar{\tilde{F}}_{31}+2\bar{\tilde{F}}'^s_{31}+\bar{\tilde{f}}'^s_{31},\\&\bar{B}_5=\bar{\tilde{Y}}_{33}+2\bar{\tilde{Y}}^s_{33}+2\bar{\tilde{g}}^s_{33},\bar{B}_6=\bar{\tilde{T}}_{33}+2\bar{\tilde{T}}^s_{33}+2\bar{\tilde{\mu}}^s_{33},\bar{B}_7=\frac{2c^s_{44}}{c_{33}h}\left(\bar{F}_{33}+2\bar{F}^s_{33}+\bar{f}^s_{33}\right),\\&\bar{B}_9=\frac{2Z_1\psi_m\phi_m}{c_{33}A_{11}h^3}\left(f_{33}+\frac{2}{b}f^s_{33}\right),\bar{B}_{10}=\frac{2Z_2\psi_m^2}{c_{33}A_{11}h^3}\left(f_{33}+\frac{2}{b}f^s_{33}\right).\end{aligned} \tag{20d}$$

Also, considering Eq. (14) the associated boundary conditions for simply supported end conditions can be expressed as follows:

$$W = \Theta = \Psi = 0, \bar{M}_x = \bar{M}_1 \frac{\partial \Phi}{\partial X} + \bar{M}_2 \eta \Theta + \bar{M}_3 \eta \Psi + \bar{M}_4 \left(\frac{1}{\eta} \frac{\partial^2 W}{\partial X^2} + \frac{\partial \Phi}{\partial X} \right) - \bar{M}_6 \frac{\partial^2 \Theta}{\partial X^2}$$
$$-\bar{M}_7 \frac{\partial^2 \Psi}{\partial X^2} + \eta \mu^2 \left(-\frac{\partial}{\partial X} \left(\bar{N}_L \frac{\partial w}{\partial X} \right) + K_w W - K_g \frac{\partial^2 W}{\partial X^2} \right) = 0, \tag{21}$$

The derivation $\bar{M}_x$ equation can be found in Appendix C.

6 SOLUTION METHOD

In this section, an analytical method is used to solve the motion equations. For this purpose, the following buckling modes are assumed to solve the governing motion equations of a simply supported PMNB (Eqs. (19)) as:

$$W = \bar{W} \sin(m\pi X), \tag{22a}$$

$$\Phi = \bar{\Phi} \cos(m\pi X), \tag{22b}$$

$$\Theta = \bar{\Theta} \sin(m\pi X), \tag{22c}$$

$$\Psi = \bar{\Psi} \sin(m\pi X), \tag{22d}$$

where $\bar{W}, \bar{\Phi}, \bar{\Theta}$ and $\bar{\Psi}$ are arbitrary dimensionless coefficients and m denotes the axial half wave number. Substituting Eqs. (22) into Eq. (19) leads to:

$$\begin{bmatrix} K_{11} & K_{12} & K_{13} & K_{14} \\ K_{21} & K_{22} & K_{23} & K_{24} \\ K_{31} & K_{32} & K_{33} & K_{34} \\ K_{41} & K_{42} & K_{43} & K_{44} \end{bmatrix} \begin{Bmatrix} \bar{W} \\ \bar{\Phi} \\ \bar{\Theta} \\ \bar{\Psi} \end{Bmatrix} = \begin{Bmatrix} 0 \\ 0 \\ 0 \\ 0 \end{Bmatrix} \Rightarrow [K]\{Y\} = \{0\}, \tag{23}$$

The nonzero solution for Eq. (23) can be obtained by setting the determinate of the coefficient matrix to zero. Therefore:

$$\det[K] = 0. \tag{24}$$

The solution of Eq. (24) yields the critical mechanical (P), electrical (ϕ_0) and magnetic (ψ_0) buckling loads.

7 VALIDATION

To the best of author's knowledge no published literature is available on the buckling analysis of PMNBs. As a result, in order to compare the results of the present study with those published on the surface effect analysis of nanobeam buckling, a simplified model is obtained by neglecting the electric and magnetic terms in Eq. (24). This simplified model is quite similar to the model developed by Ansari and Sahmani [25], although, formulations of surface layers effects in two studies are not the same. Therefore, our results for the critical mechanical buckling loads is compared with those of Ansari and Sahmani [25] as indicated in Table 1. in which a good agreement can be

found. It is important to note that a negligible difference between the results from two studies has been caused due to differences in the formulations of surface layers effects.

Table 1
Comparing the critical mechanical buckling load (*nN*) obtained in the present study and those of Ansari and Sahmani [25].

L/h	*m*=1		*m*=2		*m*=3	
	Ansari and Sahmani [25]	Present Work	Ansari and Sahmani [25]	Present Work	Ansari and Sahmani [25]	Present Work
10	1.4226	1.3472	5.3013	5.05490008	10.7081	10.3086535
15	0.6410	0.60618	2.4818	2.35472925	5.3013	5.05490008
20	0.3623	0.34246	1.4226	1.34722507	3.1058	2.95003872
25	0.2324	0.21962	0.9185	0.86911521	2.0267	1.9213841
30	0.1616	0.15268	0.6410	0.60618398	1.4226	1.34722507
35	0.1188	0.11225	0.4723	0.44653369	1.0520	0.99561572
40	0.0910	0.085977	0.3623	0.34246329	0.8089	0.76518735
45	0.0719	0.067952	0.2866	0.27090661	0.6410	0.60618398
50	0.0583	0.055053	0.2324	0.21961916	0.5203	0.4919353

8 NUMERICAL RESULTS AND DESCUSSIONS

In this section, the surface stress effects on buckling of a simply supported PMNB made from $BiTiO_3$-$CoFe_2O_4$ are illustrated and discussed. The effects of surface layer coefficients, small scale parameter, aspect ratio, surrounded elastic medium are shown graphically.

For this purpose, the exact correlation for the critical buckling loads is yielded from Eq. (24). According to Ke et al. [37], the mechanical, electrical and magnetic properties of the assumed PMNB are listed in Table 2. Moreover, the values of small scale parameter are taken in accordance with those assumed by Ke et al. [37].

Table 2
Mechanical, electrical and magnetic properties of the PMNB made from BiTiO3-CoFe2O4 [37].

Elastic constants (*GPa*)	Piezoelectric (C/m^2)	Dielectric 10^{-9} (C/Vm)	Piezomaagnetic (N/Am)	Magnetoelectric 10^{-12} (Ns/VC)	Magnetic 10^{-6} (Ns^2/C^2)
$c_{11}=226$	$e_{31}=-2.2$	$h_{11}=5.64$	$f_{31}=290.1$	$g_{11}=5.367$	$\mu_{11}=-297$
$c_{12}=125$	$e_{33}=9.3$	$h_{33}=6.35$	$f_{33}=349.9$	$g_{33}=2737.5$	$\mu_{31}=83.5$
$c_{13}=124$	$e_{15}=5.8$		$f_{15}=275$		$\mu_{33}=-297$
$c_{33}=216$					
$c_{44}=44.2$					

Based on the results presented by Gurtin and Mudoch [39], Zhang et al. [22] concluded the following relationship for surface modules (ℓ_s) and their bulk counterpart (ℓ_b) as: $\ell_s \leftrightarrow l\ell_b$,
where l is a material instinct length. In the present study, the mechanical, electrical and magnetic properties of surface layers are obtained using the mentioned relation, Also the Winkler and Pasternak constants are assumed to be $k_w = 3\times10^7\ N/m^3$ and $k_g = 2\times10^{-10}\ N/m$.

The influences of surface layers elastic coefficients for different small scale parameters are depicted in Figs. 2(a), 2(b) and 2(c) for the mechanical, electrical and magnetic critical buckling loads, respectively. A downward trend is observed Figs. 2(a) and 2(b), i.e. with an increase of small scale parameter both mechanical and electrical critical buckling loads decreases. Although the upward behavior of magnetic critical buckling load in Fig. 2(c) is in contrast with that of Figs. 2(a) and 2(b), a lower force is needed for the occurrence of buckling phenomenon in higher small scale parameter values. In the other words, due to this reality that the values of vertical axis of the Fig. 2(c) is negative, a negative magnetic load is needed to cause buckling. Therefore, in order to compare the behavior of magnetic critical buckling load with mechanical and electrical critical buckling loads, absolute values of magnetic critical buckling load should be taken into account. Motivated by these considerations, every growth in the small scale parameter contributes to a fall in the magnetic critical buckling load. Hence, one can say that the increasing of the small scale parameter decreases the energy of the system and the system becomes looser. In addition, it is seen

from Fig. 2 that the increasing of the surface layers elastic coefficients leads to a rise in the absolute values of the critical mechanical, electrical and magnetic loads. It is due to the fact that higher surface layers elastic coefficients yields stiffer structure.

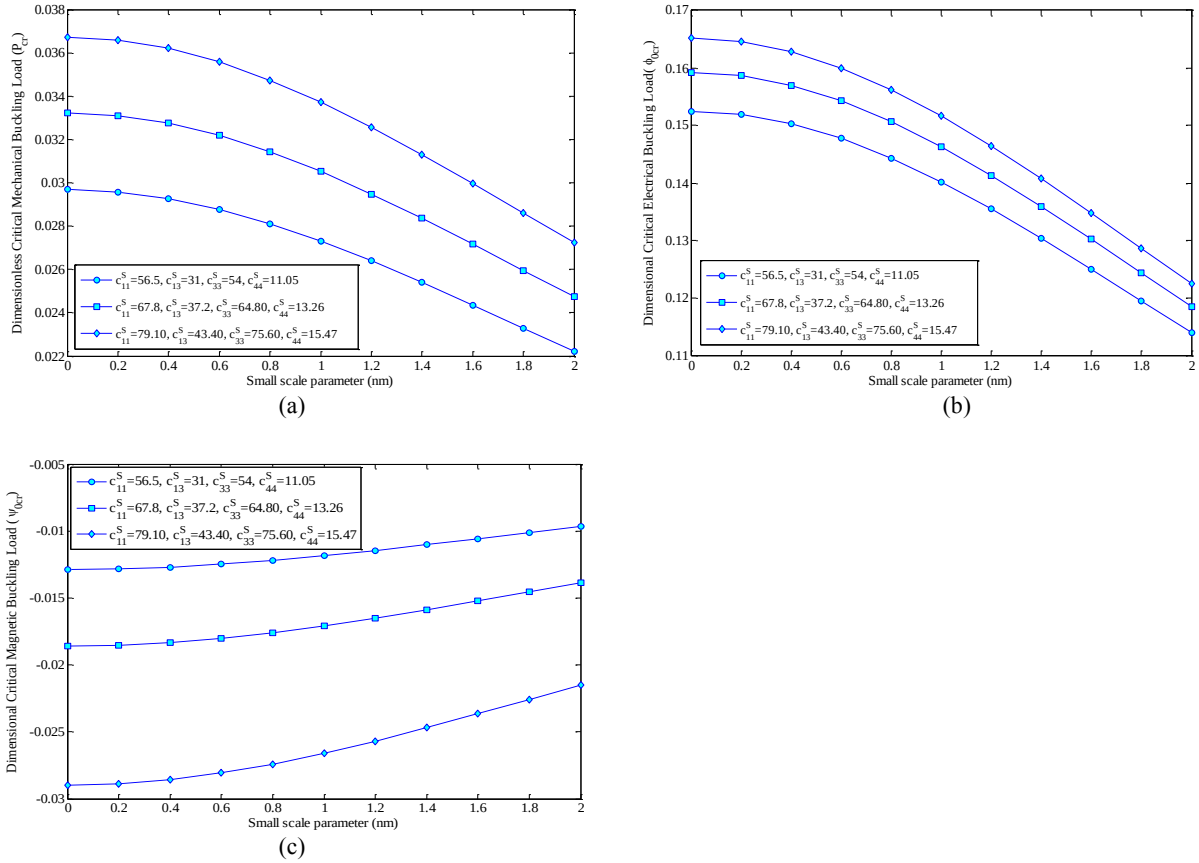

Fig.2
Surface layers elastic coefficients effects on the critical buckling loads versus small scale parameter under a) mechanical, b) electrical and c) magnetic loading.

Fig. 3 displays surface layers dielectric coefficients effects on the buckling of the PMNB. From Figs. 3(a), 3(b) and 3(c) for the mechanical, electrical and magnetic buckling loads, respectively, an increase in the dielectric surface coefficients is accompanied by a decrease in the critical buckling loads. Though, the increase of surface layers piezomagnetic coefficients decrease the absolute values of the critical buckling loads as it is shown in Figs. 4(a), 4(b) and 4(c) for the mechanical, electrical and magnetic loads, respectively.

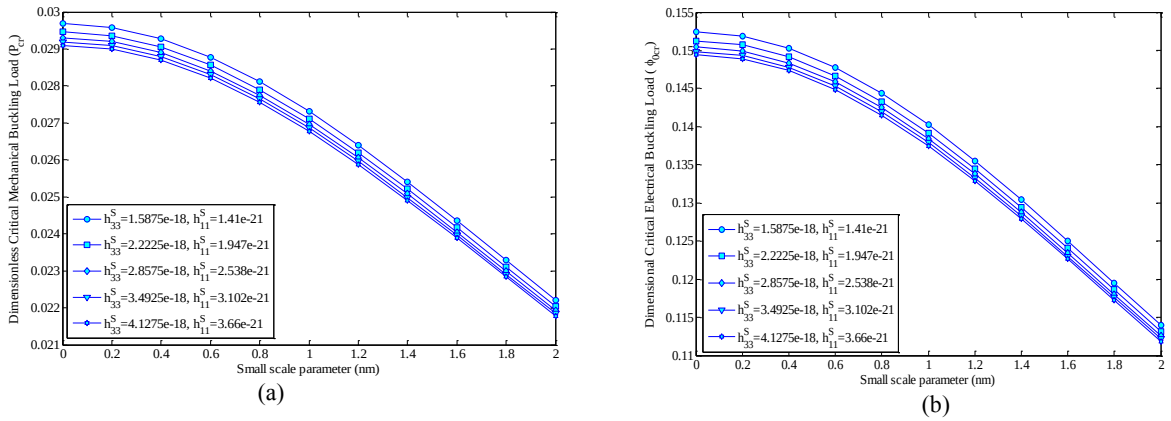

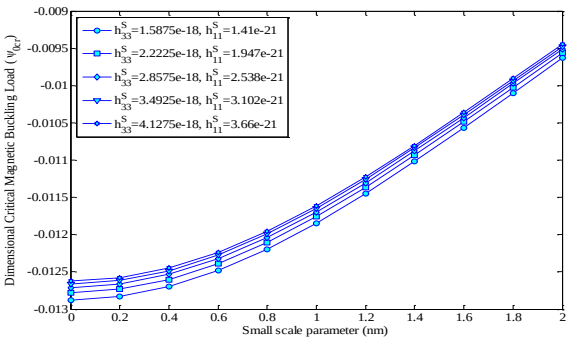

(c)

Fig.3
Surface layers dielectric coefficients effects on the critical buckling loads versus small scale parameter under a) mechanical, b) electrical and c) magnetic loading.

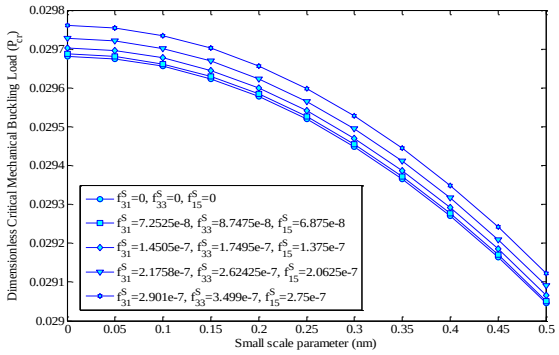

(a)

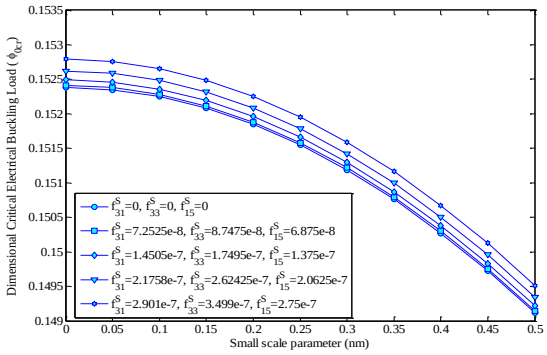

(b)

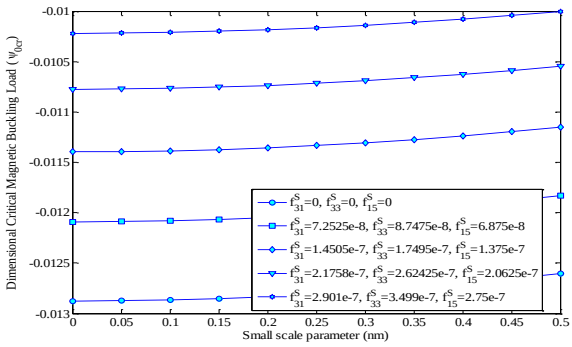

(c)

Fig.4
Surface layers piezomagnetic coefficients effects on the critical buckling loads versus small scale parameter under a) mechanical, b) electrical and c) magnetic loading.

Fig. 5 delineates the influences of surface layers piezoelectric coefficients on the buckling of the PMNB. The critical buckling loads versus aspect ratio (L/h) of the PMNB are plotted for the cases of mechanical, electrical and magnetic loadings in the Figs. 5(a), 5(b) and 5(c), respectively. It can be concluded from Fig. 5 that the increase of aspect ratio diminishes the critical buckling loads absolute values apart from the type of loading. Also, it is seen in Fig. 5(a) that a growth in the surface layers piezoelectric coefficients leads to an increase in the critical mechanical buckling load. However, a reverse behavior is true for the buckling of nanobeams under electrical and magnetic loadings, that is, increasing of the piezoelectric surface coefficient decreases the critical buckling loads. Furthermore, it is deducible from Fig. 5 that in all of the three types of loadings the differences in the buckling load in response to variation of the surface layers piezoelectric coefficients are more conspicuous at lower aspect ratio values. Hence, it is a logical conclusion that PMNBs with a lower aspect ratio are more sensitive to surface layers piezoelectric coefficients.

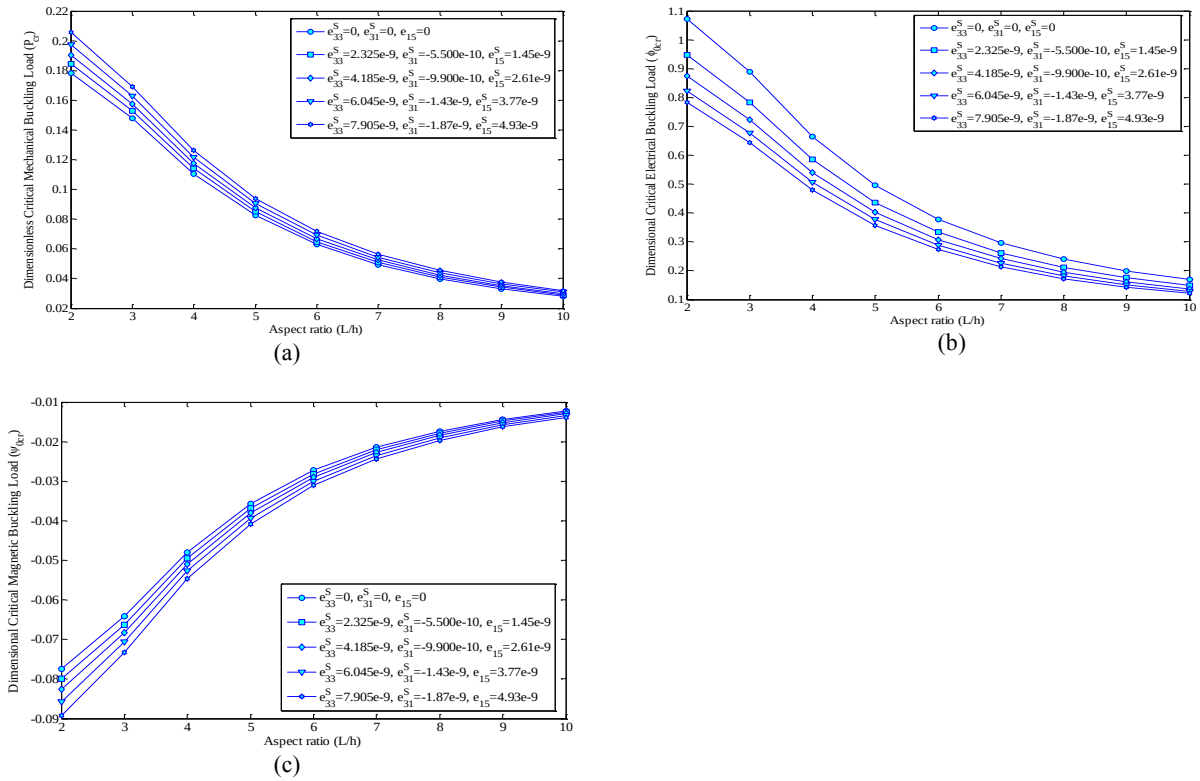

Fig.5
Surface layers piezoelectric coefficients effects on the critical buckling loads versus aspect ratio (L/h) under a) mechanical, b) electrical and c) magnetic loading.

It is likely in practical applications that the system is subjected to various types of loadings. Therefore, it is momentous to investigate the buckling of the PMNB in these circumstances to determine the share of any type in occurrence of the buckling. The results for the cases in which the PMNB is subjected to mechanical and whether electrical or magnetic forces are presented in Figs. 6-9. These figures indicate the critical mechanical load for the given values of external electric or magnetic potential. As it is observed in the figures, with the increase of the external potentials absolute critical buckling load values decreases and tend to zero.

Figs. 6(a) and 6(b), respectively, illustrate the mechanical critical buckling load corresponded to the given values of the applied external electric and magnetic potentials for different buckling mode numbers. It is clear that both mechanical critical buckling load and absolute critical external potentials increases with an increasing of the buckling mode number values.

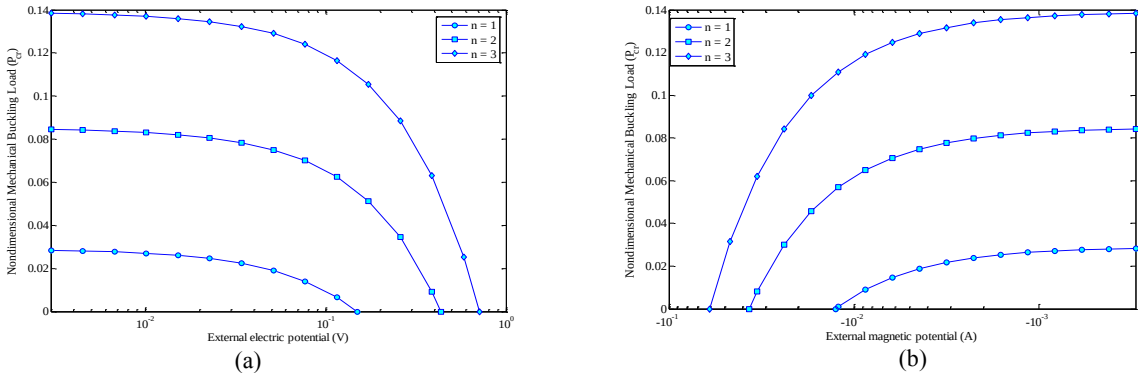

Fig.6
Mechanical critical buckling load with respect to the external applied potentials a) electric b) magnetic potential.

The effects of aspect ratio on the buckling of PMNB subjected to different types of loadings are shown in Fig. 7. It is seen form Fig. 7 that with augment of the aspect ratio mechanical, electrical and magnetic critical buckling loads dwindles.

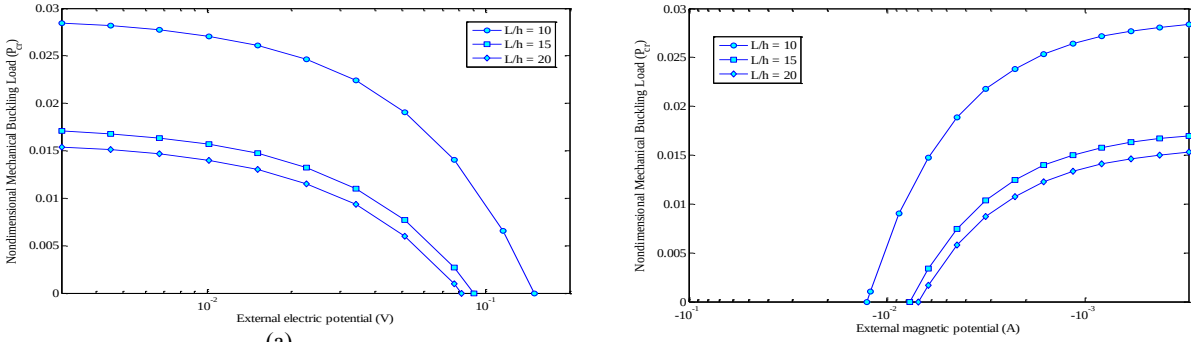

Fig.7
Effect of aspect ratio on the mechanical critical buckling of PMNB subjected to a) electric b) magnetic potential.

For various values of small scale parameters, critical mechanical buckling load versus external electrical and magnetic potentials are depicted in Figs. 8(a) and 8(b). It can be deduced from Fig. 8 that the highest mechanical critical buckling load, critical external electric potential and absolute value of the critical external magnetic potential are allocated to the classic model, small scale parameter equals to zero. With proliferation of the length scale parameter critical loads decline.

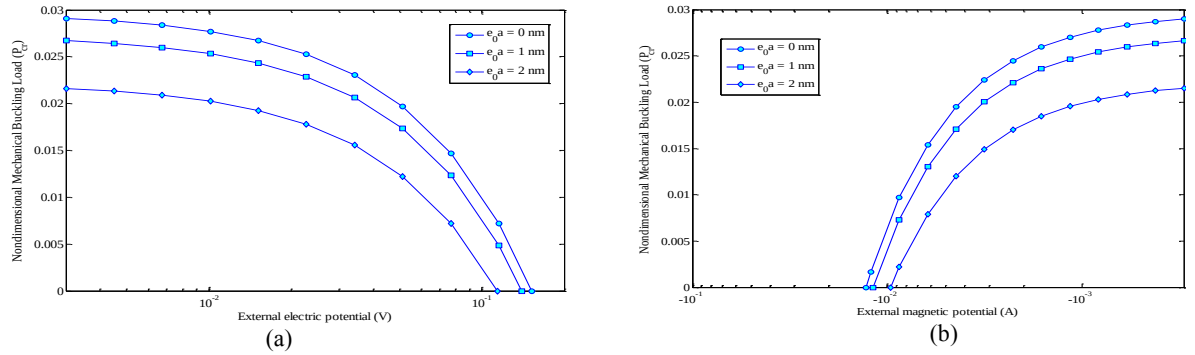

Fig.8
Effect of small scale parameter on the mechanical critical buckling of PMNB subjected to a) electric b) magnetic potential.

Fig. 9 demonstrates the effect of surface residual stress on the critical mechanical buckling load. It is observed that existence of the surface residual stress increases the mechanical load. Hence, it is possible to prevent from buckling of nanobeam with increasing surface residual stresses.

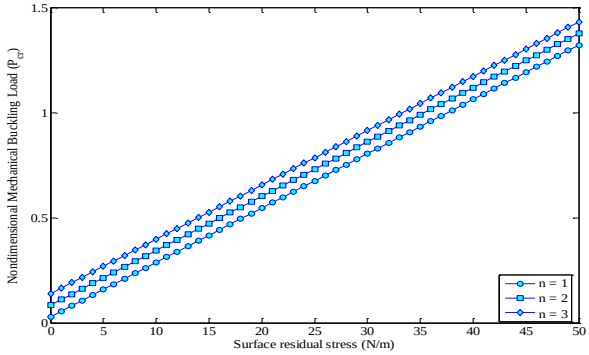

Fig.9
Effect of surface residual stress on the critical mechanical buckling load.

The effect of surrounding medium is investigated through Table 3. for different mode numbers and aspect ratio values. Tables 3(a), 3(b) and 3(c) present critical mechanical electrical and magnetic buckling loads, respectively. It is seen that Pasternak model has the highest critical buckling loads for all types of loadings in every mode number and aspect ratio. In the contrary, the lowest buckling loads are reported for the case without considering medium. In addition, with increasing the mode number and decreasing the aspect ratio, the critical buckling loads increase apart from type of the loading.

Table 3
Surrounding elastic medium effect on the dimensionless critical buckling loads a) mechanical b) electrical c) magnetic.

3a

L/h	Without Considering Medium			Winkler Medium			Pasternak Medium		
	m=1	*m*=2	*m*=3	*m*=1	*m*=2	*m*=3	*m*=1	*m*=2	*m*=3
5	0.083230	0.17066	0.18030	0.08372	0.17078	0.18036	0.08501	0.17207	0.18165
10	0.025796	0.08322	0.13748	0.02775	0.08371	0.13770	0.02905	0.08500	0.13899
15	0.011967	0.04326	0.08321	0.01638	0.04436	0.08370	0.01767	0.04565	0.08500
20	0.006835	0.02579	0.05289	0.01468	0.02775	0.05376	0.01598	0.02905	0.05505

3b

L/h	Without Considering Medium			Winkler Medium			Pasternak Medium		
	m=1	*m*=2	*m*=3	*m*=1	*m*=2	*m*=3	*m*=1	*m*=2	*m*=3
5	0.427296	0.87617	0.92568	0.42982	0.87680	0.92596	0.436448	0.88343	0.93259
10	0.132433	0.42725	0.70582	0.14251	0.42977	0.70694	0.149145	0.43640	0.71357
15	0.061439	0.22209	0.42723	0.08412	0.22776	0.42975	0.090751	0.23440	0.43639
20	0.035091	0.13243	0.27155	0.075410	0.14251	0.27603	0.082043	0.14914	0.28267

3c

L/h	Without Considering Medium			Winkler Medium			Pasternak Medium		
	m =1	*m* =2	*m* =3	*m* =1	*m* =2	*m* =3	*m* =1	*m* =2	*m* =3
5	-0.0361009	-0.074025	-0.078207	-0.0363138	-0.0740779	-0.078231	-0.0368742	-0.074638	-0.078791
10	-0.0111889	-0.036097	-0.059632	-0.0120405	-0.0363098	-0.059727	-0.0126008	-0.03687	-0.060287
15	-0.0051908	-0.018764	-0.036096	-0.0071069	-0.019243	-0.036309	-0.0076672	-0.019803	-0.036869
20	-0.0029647	-0.011189	-0.022943	-0.0063712	-0.0120403	-0.023321	-0.0069315	-0.012601	-0.023882

Tables 4(a), 4(b) and 4(c) imply the importance of surface coefficients effects on the critical mechanical, electrical and magnetic buckling loads, respectively. It is obvious that considering surface effects is accompanied by a dramatic growth in the absolute value of critical buckling loads. This trend is true for all of small scale parameters and mode numbers. An interesting conclusion from this table is that the influence of surface effects is not limited to the mechanical buckling loads and the surface layers characteristics play an undeniable role in the magnetic and electric buckling load values.

Table 4
Surface layer characteristic effects on the dimensional critical buckling loads a) mechanical (*nN*) b) electrical (*V*) c) magnetic (*A*).

4a

$e_0a(nm)$	Without consideration of surface layer characteristics			With consideration of surface layer characteristics		
	m =1	*m* =2	*m* =3	*m* =1	*m* =2	*m* =3
0	1.8019	5.0046	9.5048	4.5961	14.432	26.245
0.5	1.7706	4.5798	7.8202	4.4976	13.160	21.518
1	1.6853	3.6662	5.1436	4.2285	10.425	14.009
1.5	1.5660	2.7802	3.3256	3.8525	7.7726	8.9081
2	1.4345	2.1094	2.2700	3.4379	5.7645	5.9466

4b

$e_0a(nm)$	Without consideration of surface layer characteristics			With consideration of surface layer characteristics		
	m =1	*m* =2	*m* =3	*m* =1	*m* =2	*m* =3
0	0.11950	0.33192	0.63039	0.15241	0.47857	0.87031
0.5	0.11743	0.30374	0.51865	0.14915	0.4364	0.71357
1	0.11177	0.24315	0.34114	0.14022	0.3457	0.46455
1.5	0.10386	0.18439	0.22056	0.12775	0.25775	0.29540
2	0.09514	0.13990	0.15055	0.11400	0.19116	0.19720

4c

$e_0a(nm)$	Without consideration of surface layer characteristics			With consideration of surface layer characteristics		
	m =1	m =2	m =3	m =1	m =2	m =3
0	-0.0100966	-0.028043	-0.053259	-0.0128769	-0.040433	-0.073529
0.5	-0.0099214	-0.025662	-0.043819	-0.0126008	-0.03687	-0.060287
1	-0.0094432	-0.020543	-0.028822	-0.011847	-0.029207	-0.039248
1.5	-0.008775	-0.015578	-0.018635	-0.0107936	-0.021776	-0.024958
2	-0.0080381	-0.011820	-0.012720	-0.0096318	-0.016150	-0.016661

9 CONCLUSIONS

Investigating surface effects on the micro- and nano-structures used in MEMS/NEMs such as PMNBs can make an effective contribution to improve the design and fabrication of such devices. In this study, the surface piezomagnetoelasticity theory was applied to study the electro-magneto-mechanical buckling characteristics of PMNBs embedded in Pasternak elastic foundation. The PMNB was subjected to external electric and magnetic potentials which can be used as the controller parameters. The nonlocal piezomagnetoelasticity theory was taken into account to consider the small scale effects. Based on TB model, the governing motion equations were derived using energy method and Hamilton's principle which are the analytically solved to obtain critical mechanical, electrical and magnetic buckling loads. The following conclusions can be made through the presented results:

The stability of the system is strongly dependent on the surface layer characteristics. Therefore, in order to study the effects of surface layers in piezoelectric/magnetostrictive structures, surface piezomagnetoelasticity theory should be taken into account. Increasing the surface layer coefficients increases the critical buckling loads.

Regarding small scale effects, it was demonstrated that the critical buckling loads are decreased with increasing the small scale parameter.

With increasing of the external electric and magnetic potential absolute values, a lower mechanical load in needed for the occurrence of the buckling phenomenon. Therefore, the system becomes looser.

Increasing the elastic foundation parameters cause to increase the stability of the system.

APPENDIX A

Considering σ_{zz} in the Eqs. (7) and (8) the following relations for the stress, electric displacement and magnetic induction components for both bulk material and surface layer can be obtained as:

$$\left(1-\left(e_0a\right)^2\nabla^2\right)\sigma_{xx}^b=\tilde{c}_{11}\left(\frac{\partial u}{\partial x}+z\frac{\partial\varphi}{\partial x}+\frac{1}{2}\left(\frac{\partial w}{\partial x}\right)^2\right)-\tilde{e}_{31}\left(-\beta\sin\left(\beta z\right)\phi-\frac{2\phi_0}{h}\right)$$
$$-\tilde{f}_{31}\left(-\beta\sin\left(\beta z\right)\psi-\frac{2\psi_0}{h}\right)+\frac{c_{13}}{c_{33}}\frac{2z}{h}\left(c_{44}^s\left(\frac{\partial^2 w}{\partial x^2}+\frac{\partial\varphi}{\partial x}\right)-e_{15}^s\cos\left(\beta z\right)\frac{\partial^2\phi}{\partial x^2}-f_{15}^s\cos\left(\beta z\right)\frac{\partial^2\psi}{\partial x^2}\right), \tag{A.1}$$

$$\left(1-\left(e_0a\right)^2\nabla^2\right)\sigma_{xz}^b=c_{44}\left(\frac{\partial w}{\partial x}+\varphi\right)-e_{15}\cos\left(\beta z\right)\frac{\partial\phi}{\partial x}-f_{15}\cos\left(\beta z\right)\frac{\partial\psi}{\partial x}, \tag{A.2}$$

$$\left(1-\left(e_0a\right)^2\nabla^2\right)D_x^b=e_{15}\left(\frac{\partial w}{\partial x}+\varphi\right)+h_{11}\cos\left(\beta z\right)\frac{\partial\phi}{\partial x}+g_{11}\cos\left(\beta z\right)\frac{\partial\psi}{\partial x} \tag{A.3}$$

$$\left(1-\left(e_0a\right)^2\nabla^2\right)D_z^b=\tilde{e}_{31}\left(\frac{\partial u}{\partial x}+z\frac{\partial\varphi}{\partial x}+\frac{1}{2}\left(\frac{\partial w}{\partial x}\right)^2\right)+\tilde{h}_{33}\left(-\beta\sin\left(\beta z\right)\phi-\frac{2\phi_0}{h}\right)$$
$$+\tilde{g}_{33}\left(-\beta\sin\left(\beta z\right)\psi-\frac{2\psi_0}{h}\right)+\frac{e_{33}}{c_{33}}\frac{2z}{h}\left(c_{44}^s\left(\frac{\partial^2 w}{\partial x^2}+\frac{\partial\varphi}{\partial x}\right)-e_{15}^s\cos\left(\beta z\right)\frac{\partial^2\phi}{\partial x^2}-f_{15}^s\cos\left(\beta z\right)\frac{\partial^2\psi}{\partial x^2}\right), \tag{A.4}$$

$$\left(1-\left(e_0a\right)^2\nabla^2\right)B_x^b=f_{15}\left(\frac{\partial w}{\partial x}+\varphi\right)+g_{11}\cos\left(\beta z\right)\frac{\partial\phi}{\partial x}+\mu_{11}\cos\left(\beta z\right)\frac{\partial\psi}{\partial x},\tag{A.5}$$

$$\begin{aligned}\left(1-\left(e_0a\right)^2\nabla^2\right)B_z^b&=\tilde{f}_{31}\left(\frac{\partial u}{\partial x}+z\frac{\partial\varphi}{\partial x}+\frac{1}{2}\left(\frac{\partial w}{\partial x}\right)^2\right)+\tilde{g}_{33}\left(-\beta\sin\left(\beta z\right)\phi-\frac{2\phi_0}{h}\right)\\&+\tilde{\mu}_{33}\left(-\beta\sin\left(\beta z\right)\psi-\frac{2\psi_0}{h}\right)+\frac{f_{33}}{c_{33}}\frac{2z}{h}\left(c_{44}^s\left(\frac{\partial^2w}{\partial x^2}+\frac{\partial\varphi}{\partial x}\right)-e_{15}^s\cos\left(\beta z\right)\frac{\partial^2\phi}{\partial x^2}-f_{15}^s\cos\left(\beta z\right)\frac{\partial^2\psi}{\partial x^2}\right),\end{aligned}\tag{A.6}$$

$$\begin{aligned}\left(1-\left(e_0a\right)^2\nabla^2\right)\sigma_{xx}^s&=\sigma_{xx}^0+\tilde{c}_{11}^s\left(\frac{\partial u}{\partial x}+z\frac{\partial\varphi}{\partial x}+\frac{1}{2}\left(\frac{\partial w}{\partial x}\right)^2\right)-\tilde{e}_{31}^s\left(-\beta\sin\left(\beta z\right)\phi-\frac{2\phi_0}{h}\right)\\&-\tilde{f}_{31}^s\left(-\beta\sin\left(\beta z\right)\psi-\frac{2\psi_0}{h}\right)+\frac{c_{13}^s}{c_{33}}\frac{2z}{h}\left(c_{44}^s\left(\frac{\partial^2w}{\partial x^2}+\frac{\partial\varphi}{\partial x}\right)-e_{15}^s\cos\left(\beta z\right)\frac{\partial^2\phi}{\partial x^2}-f_{15}^s\cos\left(\beta z\right)\frac{\partial^2\psi}{\partial x^2}\right),\end{aligned}\tag{A.7}$$

$$\left(1-\left(e_0a\right)^2\nabla^2\right)\sigma_{xz}^s=\sigma_{xz}^0+c_{44}^s\left(\frac{\partial w}{\partial x}+\varphi\right)-e_{15}^s\cos\left(\beta z\right)\frac{\partial\phi}{\partial x}-f_{15}^s\cos\left(\beta z\right)\frac{\partial\psi}{\partial x},\tag{A.8}$$

$$\left(1-\left(e_0a\right)^2\nabla^2\right)D_x^s=D_x^0+e_{15}^s\left(\frac{\partial w}{\partial x}+\varphi\right)+h_{11}^s\cos\left(\beta z\right)\frac{\partial\phi}{\partial x}+g_{11}^s\cos\left(\beta z\right)\frac{\partial\psi}{\partial x},\tag{A.9}$$

$$\begin{aligned}\left(1-\left(e_0a\right)^2\nabla^2\right)D_z^s&=D_z^0+\tilde{e}_{31}^{rs}\left(\frac{\partial u}{\partial x}+z\frac{\partial\varphi}{\partial x}+\frac{1}{2}\left(\frac{\partial w}{\partial x}\right)^2\right)+\tilde{h}_{33}^s\left(-\beta\sin\left(\beta z\right)\phi-\frac{2\phi_0}{h}\right)\\&+\tilde{g}_{33}^s\left(-\beta\sin\left(\beta z\right)\psi-\frac{2\psi_0}{h}\right)+\frac{e_{33}^s}{c_{33}}\frac{2z}{h}\left(c_{44}^s\left(\frac{\partial^2w}{\partial x^2}+\frac{\partial\varphi}{\partial x}\right)-e_{15}^s\cos\left(\beta z\right)\frac{\partial^2\phi}{\partial x^2}-f_{15}^s\cos\left(\beta z\right)\frac{\partial^2\psi}{\partial x^2}\right),\end{aligned}\tag{A.10}$$

$$\left(1-\left(e_0a\right)^2\nabla^2\right)B_x^s=B_x^0+f_{15}^s\left(\frac{\partial w}{\partial x}+\varphi\right)+g_{11}^s\cos\left(\beta z\right)\frac{\partial\phi}{\partial x}+\mu_{11}^s\cos\left(\beta z\right)\frac{\partial\psi}{\partial x},\tag{A.11}$$

$$\begin{aligned}\left(1-\left(e_0a\right)^2\nabla^2\right)B_z^s&=B_z^0+\tilde{f}_{31}^{rs}\left(\frac{\partial u}{\partial x}+z\frac{\partial\varphi}{\partial x}+\frac{1}{2}\left(\frac{\partial w}{\partial x}\right)^2\right)+\tilde{g}_{33}^{rs}\left(-\beta\sin\left(\beta z\right)\phi-\frac{2\phi_0}{h}\right)\\&+\tilde{\mu}_{33}^s\left(-\beta\sin\left(\beta z\right)\psi-\frac{2\psi_0}{h}\right)+\frac{f_{33}^s}{c_{33}}\frac{2z}{h}\left(c_{44}^s\left(\frac{\partial^2w}{\partial x^2}+\frac{\partial\varphi}{\partial x}\right)-e_{15}^s\cos\left(\beta z\right)\frac{\partial^2\phi}{\partial x^2}-f_{15}^s\cos\left(\beta z\right)\frac{\partial^2\psi}{\partial x^2}\right),\end{aligned}\tag{A.12}$$

In which:

$$\begin{aligned}&\tilde{c}_{11}=c_{11}-\frac{c_{13}^2}{c_{33}},\tilde{e}_{31}=e_{31}-\frac{c_{13}e_{33}}{c_{33}},\tilde{f}_{31}=f_{31}-\frac{c_{13}f_{33}}{c_{33}},\tilde{h}_{33}=h_{33}+\frac{e_{33}^2}{c_{33}},\tilde{g}_{33}=g_{33}+\frac{e_{33}f_{33}}{c_{33}},\\&\tilde{\mu}_{33}=\mu_{33}+\frac{f_{33}^2}{c_{33}},\tilde{c}_{11}^s=c_{11}^s-\frac{c_{13}c_{13}^s}{c_{33}},\tilde{e}_{31}^s=e_{31}^s-\frac{c_{13}^se_{33}}{c_{33}},\tilde{f}_{31}^s=f_{31}^s-\frac{c_{13}^sf_{33}}{c_{33}},\tilde{e}_{31}^{rs}=e_{31}^s-\frac{c_{13}e_{33}^s}{c_{33}},\\&\tilde{h}_{33}^s=h_{33}^s+\frac{e_{33}e_{33}^s}{c_{33}},\tilde{g}_{33}^s=g_{33}^s+\frac{f_{33}e_{33}^s}{c_{33}},\tilde{f}_{31}^{rs}=f_{31}^s-\frac{c_{13}f_{33}^s}{c_{33}},\tilde{g}_{33}^{rs}=g_{33}^s+\frac{f_{33}^se_{33}}{c_{33}},\tilde{\mu}_{33}^s=\mu_{33}^s+\frac{f_{33}^sf_{33}}{c_{33}}.\end{aligned}\tag{A.13}$$

APPENDIX B

Eqs. (15) can be rewritten by using Eqs .(13b) and (13c) as follows:

$$\left(1-\left(e_0a\right)^2\nabla^2\right)N_x=\left(1-\mu^2\nabla^2\right)\left(\int_A\sigma_{xx}dA+\int_s\sigma_{xx}^s dS\right)=$$
$$\left(bA_{11}+2\tilde{c}_{11}^s\left(b+h\right)\right)\left(\frac{\partial u}{\partial x}+\frac{1}{2}\left(\frac{\partial w}{\partial x}\right)^2\right)+2\left(b+h\right)\sigma_{xx}^0-4\left(b+h\right)\left(\frac{\tilde{e}_{31}^s\phi_0}{h}-\frac{\tilde{f}_{31}^s\psi_0}{h}\right)-2b\left(\tilde{e}_{31}\phi_0+\tilde{f}_{31}\psi_0\right), \tag{B.1}$$

$$M_x=bM_1\frac{\partial\varphi}{\partial x}+bM_2\phi+bM_3\psi+bM_4\left(\frac{\partial^2 w}{\partial x^2}+\frac{\partial\varphi}{\partial x}\right)-bM_6\frac{\partial^2\phi}{\partial x^2}-bM_7\frac{\partial^2\psi}{\partial x^2}$$
$$+\left(e_0a\right)^2\left(-\frac{\partial}{\partial x}\left(N_x\frac{\partial w}{\partial x}\right)+k_w w-k_g\frac{\partial^2 w}{\partial x^2}\right), \tag{B.2}$$

$$Q_x=bQ_1\left(\frac{\partial w}{\partial x}+\varphi\right)-bQ_2\frac{\partial\phi}{\partial x}-bQ_3\frac{\partial\psi}{\partial x}+2\sigma_{xz}^0\left(b+h\right)+\left(e_0a\right)^2\left(-\frac{\partial^2}{\partial x^2}\left(N_x\frac{\partial w}{\partial x}\right)+k_w\frac{\partial w}{\partial x}-k_g\frac{\partial^3 w}{\partial x^3}\right), \tag{B.3}$$

$$\left(1-\left(e_0a\right)^2\nabla^2\right)\left(\int_A D_x\cos\left(\beta z\right)dA+\int_S D_x\cos\left(\beta z\right)dS\right)=bD_1\left(\frac{\partial w}{\partial x}+\varphi\right)+bD_2\frac{\partial\phi}{\partial x}+bD_3\frac{\partial\psi}{\partial x}, \tag{B.4}$$

$$\left(1-\left(e_0a\right)^2\nabla^2\right)\left(\left(\int_A D_z\cos\left(\beta z\right)dA+\int_S D_z\cos\left(\beta z\right)dS\right)\right)=bD_4\frac{\partial\varphi}{\partial x}-bD_5\phi-bD_6\psi$$
$$+bD_7\left(\frac{\partial^2 w}{\partial x^2}+\frac{\partial\varphi}{\partial x}\right)-bD_9\frac{\partial^2\phi}{\partial x^2}-bD_{10}\frac{\partial^2\psi}{\partial x^2}, \tag{B.5}$$

$$\left(1-\left(e_0a\right)^2\nabla^2\right)\left(\left(\int_A B_x\cos\left(\beta z\right)dA+\int_S B_x\cos\left(\beta z\right)dS\right)\right)=bB_1\left(\frac{\partial w}{\partial x}+\varphi\right)+bB_2\frac{\partial\phi}{\partial x}+bB_3\frac{\partial\psi}{\partial x}, \tag{B.6}$$

$$\left(1-\left(e_0a\right)^2\nabla^2\right)\left(\int_A B_z\beta\sin\left(\beta z\right)dA+\int_S B_z\beta\sin\left(\beta z\right)dS\right)=bB_4\frac{\partial\varphi}{\partial x}-bB_5\phi-bB_6\psi$$
$$+bB_7\left(\frac{\partial^2 w}{\partial x^2}+\frac{\partial\varphi}{\partial x}\right)-bB_9\frac{\partial^2\phi}{\partial x^2}-bB_{10}\frac{\partial^2\psi}{\partial x^2}, \tag{B.7}$$

where:

$$M_1=D_{11}+\frac{h^2}{2}\tilde{c}_{11}^s+\tilde{c}_{11}^s\frac{h^3}{6b},M_2=\tilde{E}_{31}+h\tilde{e}_{31}^s\beta+\frac{2}{b}\tilde{E}_{31}^s,M_3=\tilde{F}_{31}+h\tilde{f}_{31}^s\beta+\frac{2}{b}\tilde{F}_{31}^s,$$
$$M_4=c_{44}^s\left(\frac{h^2}{6}\frac{c_{13}}{c_{33}}+h\frac{c_{13}^s}{c_{33}}+\frac{c_{13}^s}{c_{33}}\frac{h^2}{3b}\right),M_6=\frac{2}{h}\frac{c_{13}}{c_{33}}E_{25}^s+\frac{c_{13}^s}{c_{33}}\frac{4}{bh}E_{25}^s,M_7=\frac{2}{h}\frac{c_{13}}{c_{33}}F_{25}^s+\frac{c_{13}^s}{c_{33}}\frac{4}{bh}F_{25}^s, \tag{B.8}$$

$$Q_1=k_sA_{44}+2c_{44}^s\frac{\left(b+h\right)}{b},Q_2=k_sE_{15}+\frac{2}{b}E_{15}^s,Q_3=k_sF_{15}+\frac{2}{b}F_{15}^s, \tag{B.9}$$

$$D_1 = E_{15} + \frac{2E^s_{15}}{b}, D_2 = X_{11} + \frac{2X^s_{11}}{b}, D_3 = Y_{11} + \frac{2Y^s_{11}}{b}, D_4 = \tilde{E}_{31} + \frac{2\tilde{E}'^s_{31}}{b} + h\beta\tilde{e}'^s_{31},$$
$$D_5 = \tilde{X}_{33} + \frac{2\tilde{X}^s_{33}}{b} + 2\beta^2\tilde{h}_{33}, D_6 = \tilde{Y}_{33} + \frac{2\tilde{Y}^s_{33}}{b} + 2\beta^2\tilde{g}_{33}, D_7 = c^s_{44}\left(\frac{2}{h}\frac{E_{33}}{c_{33}} + \frac{4}{bh}\frac{E^s_{33}}{c_{33}} + 2\beta\frac{e^s_{33}}{c_{33}}\right), \tag{B.10}$$
$$D_9 = \frac{e_{33}}{c_{33}}\frac{2}{h}Z_1 + \frac{e^s_{33}}{c_{33}}\frac{4}{bh}Z_1, D_{10} = \frac{e_{33}}{c_{33}}\frac{2}{h}Z_2 + \frac{e^s_{33}}{c_{33}}\frac{4}{bh}Z_2$$

$$B_1 = F_{15} + \frac{2F^s_{15}}{b}, B_2 = Y_{11} + \frac{2Y^s_{11}}{b}, B_3 = T_{11} + \frac{2T^s_{11}}{b}, B_4 = \tilde{F}_{31} + \frac{2\tilde{F}'^s_{31}}{b} + h\beta\tilde{f}'^s_{31},$$
$$B_5 = \tilde{Y}_{33} + \frac{2\tilde{Y}'_{33}}{b} + 2\beta^2\tilde{g}'^s_{33}, B_6 = \tilde{T}_{33} + \frac{2\tilde{T}^s_{33}}{b} + 2\beta^2\tilde{\mu}^s_{33}, B_7 = c^s_{44}\left(\frac{2}{h}\frac{F_{33}}{c_{33}} + \frac{4}{bh}\frac{F^s_{33}}{c_{33}} + 2\beta\frac{f^s_{33}}{c_{33}}\right), \tag{B.11}$$
$$B_9 = \frac{f_{33}}{c_{33}}\frac{2}{h}Z_1 + \frac{f^s_{33}}{c_{33}}\frac{4}{bh}Z_1, B_{10} = \frac{f_{33}}{c_{33}}\frac{2}{h}Z_2 + \frac{f^s_{33}}{c_{33}}\frac{4}{bh}Z_2.$$

APPENDIX C

In order to find the $\bar{M}_x$ equation, one can rewrite Eq. (15b) as follows:

$$M_x = \left(bD_{11} + \frac{bh^2}{2}\tilde{c}^s_{11} + \tilde{c}^s_{11}\frac{h^3}{6}\right)\frac{\partial\varphi}{\partial x} + \left(b\tilde{E}_{31} + bh\tilde{e}^s_{31}\beta + 2\tilde{E}^s_{31}\right)\phi + \left(b\tilde{F}_{31} + bh\tilde{f}^s_{31}\beta + 2\tilde{F}^s_{31}\right)\psi$$
$$+\left(\frac{bh^2}{6}\frac{c_{13}}{c_{33}} + bh\frac{c^s_{13}}{c_{33}} + \frac{c^s_{13}}{c_{33}}\frac{h^2}{3}\right)c^s_{44}\left(\frac{\partial^2 w}{\partial x^2} + \frac{\partial\varphi}{\partial x}\right) - \left(\frac{2b}{h}\frac{c_{13}}{c_{33}}E^s_{25} + \frac{c^s_{13}}{c_{33}}\frac{4}{h}E^s_{25}\right)\frac{\partial^2\phi}{\partial x^2} \tag{C.1}$$
$$-\left(\frac{2b}{h}\frac{c_{13}}{c_{33}}F^s_{25} + \frac{c^s_{13}}{c_{33}}\frac{4}{h}F^s_{25}\right)\frac{\partial^2\psi}{\partial x^2} + (e_0a)^2\frac{\partial^2 M_x}{\partial x^2}$$

Also, from Eq. (13c) the following relation may be obtained as:

$$\frac{\partial M_x}{\partial x} - Q_x = 0 \Rightarrow \frac{\partial^2 M_x}{\partial x^2} = \frac{\partial Q_x}{\partial x} \tag{C.2}$$

Using Eq. (13b) into Eq. (C.2) yields:

$$\frac{\partial^2 M_x}{\partial x^2} = k_w w - k_g\frac{\partial^2 w}{\partial x^2} - \frac{\partial}{\partial x}\left(N_x\frac{\partial w}{\partial x}\right), \tag{C.3}$$

Substituting Eq. (C.3) into Eq. (C.1) and using dimensionless parameter (Eqs. (17)) results the $\bar{M}_x$ as expressed in Eq. (21).

ACKNOWLEDGEMENTS

The author would like to thank the reviewers for their comments and suggestions to improve the clarity of this article. This work was supported by University of Kashan [grant number 574600/40].

REFERENCES

[1] Eringen A.C., 1983, On differential equations of nonlocal elasticity and solutions of screw dislocation and surface waves, *Journal of Applied Physics* **54**: 4703-4710.

[2] Aydogdu M., 2009, A general nonlocal beam theory: Its application to nanobeam bending, buckling and vibration, *Physica E* **41**: 1651-1655.

[3] Thai H.T., 2012, A nonlocal beam theory for bending, buckling, and vibration of nanobeams, *International Journal of Engineering Science* **52**: 56-64.

[4] Nazemnezhad R., Hosseini-Hashemi S., 2014, Nonlocal nonlinear free vibration of functionally graded nanobeams, *Composite Structure* **110**: 192-199.

[5] Rahmani O., Pedram O., 2014, Analysis and modeling the size effect on vibration of functionally graded nanobeams based on nonlocal Timoshenko beam theory, *International Journal of Engineering Science* **77**: 55-70.

[6] Marotti de Sciarra F., Barretta R., 2014, A gradient model for Timoshenko nanobeams, *Physica E* **62**: 1-9.

[7] Akgöz B., Civalek Ö., 2013, A size-dependent shear deformation beam model based on the strain gradient elasticity theory, *International Journal of Engineering Science* **70**: 1-14.

[8] Mohammad Abadi M., Daneshmehr A.R., 2014, Size dependent buckling analysis of microbeams based on modified couple stress theory with high order theories and general boundary conditions, *International Journal of Engineering Science* **74**: 1-14.

[9] Muralt P., 2001, Piezoelectric thin films for MEMS, *Encyclopedia of Materials: Science and Technology* 6999-7008.

[10] Nabar B.P., Çelik-Butler Z., Butler D.P., 2014, Piezoelectric ZnO nanorod carpet as a NEMS vibrational energy harvester, *Nano Energy* **10**: 71-82.

[11] Falconi C., Mantini G., D'Amico A., Wang Z.L., 2009, Studying piezoelectric nanowires and nanowalls for energy harvesting, *Sensors and Actuators B* **139**: 511-519.

[12] Sun C., Shi J., Wang X., 2010, Fundamental study of mechanical energy harvesting using piezoelectric nanostructures, *Journal of Applied Physics* **108**: 034309.

[13] Ghorbanpour Arani A., Abdollahian M., Kolahchi R., Rahmati A.H., 2013, Electro-thermo-torsional buckling of an embedded armchair DWBNNT using nonlocal shear deformable shell model, *Composites Part B* **51**: 291-299.

[14] Chen C., Li S., Dai L., Qian C.Z., 2014, Buckling and stability analysis of a piezoelectric viscoelastic nanobeam subjected to van der Waals forces, *Communications in Nonlinear Science and Numerical Simulation* **19**: 1626-1637.

[15] Asemi S.R., Farajpour A., Mohammadi M., 2014, Nonlinear vibration analysis of piezoelectric nanoelectromechanical resonators based on nonlocal elasticity theory, *Composite Structures* **116**: 703-712.

[16] Pradhan S.C., Reddy G.K., 2011, Buckling analysis of single walled carbon nanotube on Winkler foundation using nonlocal elasticity theory and DTM, *Computational Materials Science* **50**: 1052-1056.

[17] Han Q., Lu G., 2003, Torsional buckling of a double-walled carbon nanotube embedded in an elastic medium, *European Journal of Mechanics-A/Solids* **22**: 875-883.

[18] Rahmati A.H., Mohammadimehr M., 2014, Vibration analysis of non-uniform and non-homogeneous boron nitride nanorods embedded in an elastic medium under combined loadings using DQM, *Physica B* **440**: 88-98.

[19] Abdollahian A., Ghorbanpour Arani A., Mosallaei Barzoki A.A., Kolahchi, R., Loghman A., 2013, Non-local wave propagation in embedded armchair TWBNNTs conveying viscous fluid using DQM, *Physica B* **418**: 1-15.

[20] Zenkour A.M., Sobhy M., 2013, Nonlocal elasticity theory for thermal buckling of nanoplates lying on Winkler–Pasternak elastic substrate medium, *Physica E* **53**: 251-259.

[21] Moshtaghin A.F., Naghdabadi R., Asghari M., 2012, Effects of surface residual stress and surface elasticity on the overall yield surfaces of nanoporous materials with cylindrical nanovoids, *Mechanics of Materials* **51**: 74-87.

[22] Zhang C.h., Chen W., Zhang C.h., 2012, On propagation of anti-plane shear waves in piezoelectric plates with surface effect, *Physics Letters A* **376**: 3281-3286.

[23] Zhang L.L., Liu J.X., Fang X.Q., Nie G.Q., 2014, Effects of surface piezoelectricity and nonlocal scale on wave propagation in piezoelectric nanoplates, *European Journal of Mechanics-A/Solids* **46**: 22-29.

[24] Hosseini-Hashemi S., Nazemnezhad R., Bedroud M., 2014, Surface effects on nonlinear free vibration of functionally graded nanobeams using nonlocal elasticity, *Applied Mathematical Modelling* **38**: 3538-3553.

[25] Ansari R., Sahmani S., 2011, Bending behavior and buckling of nanobeams including surface stress effects corresponding to different beam theories, *International Journal of Engineering Science* **49**: 1244-1255.

[26] Reddy K.S.M., Estrine E.C., Lim D.H., Smyrl W.H., Stadler B.J.H., 2012, Controlled electrochemical deposition of magnetostrictive Fe1-xGax alloys, *Electrochemistry Communications* **18**: 127-130.

[27] Guo J., Moritaa S., Yamagataa Y., Higuchi T., 2013, Magnetostrictive vibrator utilizing iron–cobalt alloy, *Sensors and Actuators A* **200**: 101-106.

[28] Wang H., Zhang Z.D., Wu R.Q., Sun L.Z., 2013, Large-scale first-principles determination of anisotropic mechanical properties of magnetostrictive Fe–Ga alloys, *Acta Materialia* **61**: 2919-2925.

[29] Espinosa-Almeyda Y., Rodríguez-Ramos R., Guinovart-Díaz R., Bravo-Castillero J., López-Realpozo J.C., Camacho-Montes H., Sabina F.J., Lebon F., 2014, Antiplane magneto-electro-elastic effective properties of three-phase fiber composites, *International Journal of Solids and Structures* **51**: 3508-3521.

[30] Elloumi R., Kallel-Kamoun I., El-Borgi S., Guler M.A., 2014, On the frictional sliding contact problem between a rigid circular conducting punch and a magneto-electro-elastic half-plane, *International Journal of Mechanical Sciences* **87**: 1-17.

[31] Ma J., Ke L.L., Wang Y.S., 2014, Frictionless contact of a functionally graded magneto-electro-elastic layered half-plane under a conducting punch, *International Journal of Solids and Structures* **51**: 2791-2806.

[32] Wei J., Su X., 2008, Transient-state response of wave propagation in magneto-electro-elastic square column, *Acta Mechanica Solida Sinica* **21**: 491-499.

[33] Lang Z., Xuewu L., 2013, Buckling and vibration analysis of functionally graded magneto-electro-thermo-elastic circular cylindrical shells, *Applied Mathematical Modelling* **37**: 2279-2292.

[34] Li Y.S., 2014, Buckling analysis of magnetoelectroelastic plate resting on Pasternak elastic foundation, *Mechanics Research Communications* **56**: 104-114.

[35] Razavi S., Shooshtari A., 2015, Nonlinear free vibration of magneto-electro-elastic rectangular plates, *Composite Structures* **119**: 377-384.

[36] Li Y.S., Cai Z.Y., Shi S.Y., 2014, Buckling and free vibration of magnetoelectroelastic nanoplate based on nonlocal theory, *Composite Structures* **111**: 522-529.

[37] Ke L.L., Wang Y.S., 2014, Free vibration of size-dependent magneto-electro-elastic nanobeams based on the nonlocal theory, *Physica E* **63**: 52-61.

[38] Ghorbanpour Arani A., Abdollahian M., Kolahchi R., 2014, Nonlinear vibration of embedded smart composite microtube conveying fluid based on modified couple stress theory, *Polymer Composites* **36**: 1314-1324.

[39] Gurtin M.E., Murdoch A.I., 1957, A continuum theory of elastic material surface, *Archived for Rational Mechanics Analysis* **57**: 291-323.

[40] Ansari R., Mohammadi V., Faghih Shojaei M., Gholami R., Sahmani S., 2013, Postbuckling characteristics of nanobeams based on the surface elasticity theory, *Composites part B* **55**: 240-246.

[41] Lu P., He L.H., Lee H.P., Lu C., 2006, Thin plate theory including surface effects, *International Journal of Solids and Structures* **43**: 4631-4647.